Ultra-high field MRI: Advancing systems neuroscience towards mesoscopic human brain function

Dumoulin, Serge O.; Fracasso, Alessio; van der Zwaag, Wietske; Siero, Jeroen C.W.; Petridou, Natalia

published in
NeuroImage
2018

DOI (link to publisher)
10.1016/j.neuroimage.2017.01.028

document version
Publisher's PDF, also known as Version of record

NeuroImage 168 (2018) 345–357

Contents lists available at ScienceDirect

NeuroImage

journal homepage: www.elsevier.com/locate/neuroimage

Ultra-high field MRI: Advancing systems neuroscience towards mesoscopic human brain function

Serge O. Dumoulin[a,b,*], Alessio Fracasso[a,b,c], Wietske van der Zwaag[a], Jeroen C.W. Siero[a,c], Natalia Petridou[c]

[a] Spinoza Centre for Neuroimaging, Amsterdam, Netherlands
[b] Experimental Psychology, Helmholtz Institute, Utrecht University, Utrecht, Netherlands
[c] Radiology, University Medical Centre Utrecht, Utrecht, Netherlands

ARTICLE INFO

Keywords:
Ultra-high field
7 T
MRI
Cortical organization
Cortical processing unit
Hypercolumn

ABSTRACT

Human MRI scanners at ultra-high magnetic field strengths of 7 T and higher are increasingly available to the neuroscience community. A key advantage brought by ultra-high field MRI is the possibility to increase the spatial resolution at which data is acquired, with little reduction in image quality. This opens a new set of opportunities for neuroscience, allowing investigators to map the human cortex at an unprecedented level of detail. In this review, we present recent work that capitalizes on the increased signal-to-noise ratio available at ultra-high field and discuss the theoretical advances with a focus on sensory and motor systems neuroscience. Further, we review research performed at sub-millimeter spatial resolution and discuss the limits and the potential of ultra-high field imaging for structural and functional imaging in human cortex. The increased spatial resolution achievable at ultra-high field has the potential to unveil the fundamental computations performed within a given cortical area, ultimately allowing the visualization of the mesoscopic organization of human cortex at the functional and structural level.

Introduction

The human brain and, in particular, the cerebral cortex, holds the key to who we are, our memories, thoughts and perception of the world around us. Human cortex is organized at different spatial scales, ranging from the few micrometres of an individual neuron (microscopic scale), to cortical columns and cortical layers at the millimetre scale (mesoscopic scale) and the several centimetres covered by cortical areas and white matter tracts (macroscopic scale). Obviously, to understand our brain, its disorders and ultimately ourselves, requires knowledge of neuronal operations at all length scales.

Several methods exist that measure the brain at different spatial scales (Fig. 1). At the microscopic scale, Hubel and Wiesel pioneered measurements at the single neuron level using non-human invasive electrophysiology (Hubel and Wiesel, 1959). Together with Mountcastle (1957), they used the same invasive animal techniques to provide a first description of the functional properties of the mesoscopic organization scale of visual and somatosensory cortex. At the mesoscopic scale they described novel columnar structures, where columns refer to the vertical organization of structures within the cortex where neurons have similar functional properties. Although they pioneered these measurements, they described their micro-electrode experiments as: “to attack such a three-dimensional problem with a one-dimensional weapon is a dismaying exercise in tedium, like trying to cut the back lawn with a pair of nail scissors” (Hubel and Wiesel, 1977). While these techniques pioneered the identification of mesoscopic organisation in non-human animals, they are clearly not ideal to measure the brain's organization and function at the mesoscopic scale. Further developments of invasive optical imaging techniques, confirmed and extended the observation of columnar organization (Bonhoeffer and Grinvald, 1991; Grinvald et al., 1986; Ts'o et al., 1990) but these techniques are restricted to non-human animals and relatively flat pieces of cortex near the surface of the brain.

At the macroscopic scale, non-invasive human neuroimaging measures neuronal properties at the level of brain areas, in particular Magnetic Resonance Imaging (MRI) and functional MRI. MRI has rapidly become the most popular technique to study the living human brain. Part of the popularity of MRI is its diversity; MRI can be used to study the brain from anatomical, functional, connectivity and chemical compositional aspects. Functional MRI, in particular, allowed researchers to segregate the human cortex into different regions, a few centimetres apart. Numerous cortical areas have been identified, either

* Corresponding author at: Spinoza Centre for Neuroimaging, Meibergdreef 75, 1105 BK Amsterdam, The Netherlands.
E-mail address: s.dumoulin@spinozacentre.nl (S.O. Dumoulin).

http://dx.doi.org/10.1016/j.neuroimage.2017.01.028
Received 4 September 2016; Accepted 12 January 2017
Available online 16 January 2017
1053-8119/

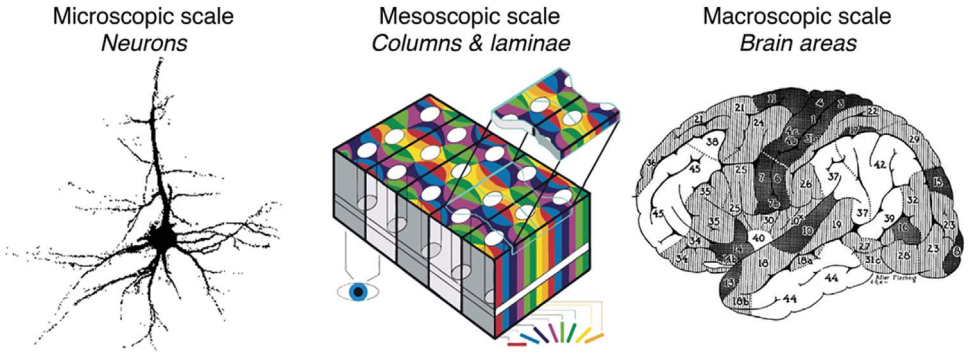

Fig. 1. Different organization scales of the human brain, ranging from microscopic to mesoscopic to macroscopic. Conventional MRI typically operates as the macroscopic level of brain areas. The image here shows the brain areas as defined by myeloarchitecture (adapted from (Flechsig, 1901). Advances in structural imaging at ultra-high field may ultimately yield similar area delineations based on structural myelin-weighted images. Ultra-high field MRI opens the neuroscience field towards imaging at the human mesoscopic scale. This scale contains the hypercolumn (Hubel and Wiesel, 1977) that where individual neurons with similar functions are organized into columnar and laminar structures that reflect the fundamental computations of a given area (adapted from Grinvald et al., 1999).

by their topographic organization or their functional specialization, and each area is believed to support a specific function or computation (Dumoulin, 2015; Grill-Spector and Malach, 2004; Op de Beeck et al., 2008; Tootell et al., 1996; Vanduffel et al., 2014; Wandell et al., 2007). In this review, we will predominantly focus on functional advances and touch on some anatomical advances in systems neuroscience.

One of the most basic developments in the field of MRI has been the increase in the static magnetic field strength (B0): from initial experiments at field strengths of 1.5 T to high field of 3 and 4 T to ultra-high field strengths of 7 T and beyond. As the available magnetization increases with increasing field strength, the primary advantage of increased field strengths is increased signal-to-noise ratios. This primary advantage can be traded off for increased spatial resolution or to advance other aspects of the MRI measurements. However, here we argue that the fundamental advantage of ultra-high field MRI for neuroscience is not only the increased signal-to-noise ratio but the ability to visualize a new organization level of the human brain at the mesoscopic scale.

At the mesoscopic scale, laminar and columnar organizations arise. Besides laminae and columns, this mesoscopic organization scale has been proposed to hold the “hypercolumn”. The hypercolumn contains all the different laminae and columns of a given area or, in other words, a hypercolumn contains all the different types of neurons that perform the basic computations of that given area. As put by Hubel and Wiesel in visual cortex: a hypercolumn contains “all the cortical machinery required to process visual information in all possible ways for a given point in visual space” (Hubel and Wiesel, 1977) and is “a complete array of columns as a small machine that looks after all values of a given variable” (Hubel and Wiesel, 1974). Their proposal was based on measurements in non-human primary visual cortex. We propose that this hypercolumn reflects the computational unit of the cortex or cortical processing unit (CPU). This notion is analogous to the central processing unit in computers, which is the electronic circuitry within a computer that performs the basic arithmetic, logical, control and input/output operations. We hypothesize that neurons organize themselves into similar processing units that may be found throughout the brain. We expect these CPU's to differ according to the computations a given area performs. Should this hypothesis be verified, this would make the identification, description and function of these processing units one of the most critical endeavours to understand the human brain and it will make the mesoscopic scale one of the most important scales of neuroscience. We hypothesize that neurons organize themselves into similar processing units that may be found throughout the brain (Mountcastle, 1978; Rockel et al., 1980).

In this review, we will cover the advances that have been made with ultra-high field MRI. First, we will briefly cover advances at more conventional spatial resolutions (> 1 mm) that capitalize on the improved signal and contrast to noise ratios of ultra-high field MRI. Second, we will discuss the advances to measure mesoscopic organization scale at high spatial resolution (< 1 mm) from methodological and neuronal, i.e. laminar and columnar, perspectives.

Ultra-high field MRI at conventional spatial resolutions (> 1 mm)

As the available magnetization increases with increasing field strength, the principal advantage of ultra-high field MRI systems is the increased signal-to-noise ratio (Edelstein et al., 1986). However, in functional neuroimaging, the timecourses are important, not necessarily the images themselves. Hence, the achievable temporal signal-to-noise ratio, tSNR, is much more important than the image SNR, and this measure of temporal stability depends on a number of factors besides the image SNR, such as system stability, physiological noise contributions and data analysis (Jorge et al., 2013; Kruger and Glover, 2001; Triantafyllou et al., 2006). It is clear however, that increases in field strength also tend to bring net tSNR advantages, especially at higher spatial resolutions (Triantafyllou et al., 2005) (Fig. 2). In

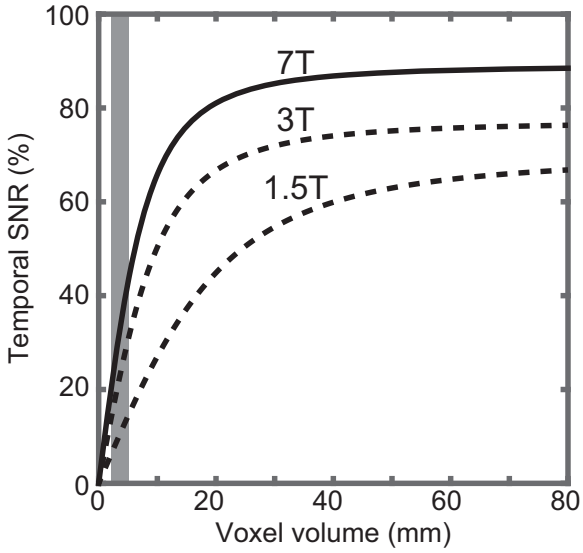

Fig. 2. Temporal signal to noise (tSNR) ratios for three different field strengths as a function of voxel volume for T2*-weighted functional imaging. Ultra-high field MRI (7 T) has improved sensitivity and of particular relevance is the improvement at small voxel volumes approximately at the mesoscopic spatial scale (vertical gray bar). Drawn after (Triantafyllou et al., 2005).

addition, the amplitude of the BOLD responses increases supralinearly with field strength (van der Zwaag et al., 2009a; Yacoub et al., 2001), while the venous contribution is reduced because of the short venous T_2^* (Koopmans et al., 2008; van der Zwaag et al., 2015b), leading to larger, and more tissue-specific functional responses. Specifically, at lower field strengths (< 3 T) intravascular BOLD signals dominate whereas at ultra-high field strength extravascular signals dominate (Boxerman et al., 1995a; Duong et al., 2003; Lu and Van Zijl, 2005; Uludağ et al., 2009). Therefore, at ultra-high field strengths, we observe a large relative increase in microvascular contributions due to diminished intravascular signals from large venous vessels (Kim and Ogawa, 2012; Uludağ et al., 2009; Yacoub et al., 2001). This significantly increases the spatial specificity of BOLD fMRI. In short, ultra-high field functional MRI provides both an increased sensitivity and specificity.

This combination of increased (t)SNR and BOLD contrast has been exploited in a fast-expanding series of sensory and motor systems neuroscience fMRI studies, including topographic maps in retinotopic (Hoffmann et al., 2009; Olman et al., 2010; Sanchez-Panchuelo et al., 2012), tonotopic (Da Costa et al., 2011; Formisano et al., 2003) and somatotopic (Martuzzi et al., 2014; Sanchez-Panchuelo et al., 2010) cortex. These topographic maps reflect the layout of the corresponding sensory or motor organ, e.g. retina or cochlea, whereas no such organs exist for cognitive functions. Ultra-high field fMRI in combination with biologically-inspired data-analyses (Dumoulin and Wandell, 2008) lead to the discovery of the first topographic maps that do not represent a sensory or motor organ but an abstract dimension (Harvey et al., 2013, 2015). These topographic maps represent non-symbolic magnitudes (or quantities) in an orderly fashion, akin to non-symbolic number lines in our brain. These specific magnitudes reflect the item number (numerosity) (Harvey et al., 2013) and item size (Harvey et al., 2015). This finding put forward the hypothesis that the computational benefits of topographic maps, i.e. the close proximity and orderly topography of neurons with similar functional roles, apply to higher-order cognitive functions and sensory-motor functions alike.

Further ultra-high field MRI approaches explored the principles of topographic organization as it changes from retinal to cyclopean representation (Barendregt et al., 2015), with attention (Da Costa et al., 2013; Klein et al., 2014) or as a function of variable stimulus and action properties (Beckett et al., 2012; Gutteling et al., 2015; Harvey and Dumoulin, 2016; Kolasinski et al., 2016; Martuzzi et al., 2015; Moerel et al., 2015; Thunell et al., 2016; van der Zwaag et al., 2015a). Furthermore, ultra-high field MRI has also been used to characterize the plasticity and stability of topographic maps in visual cortex following congenital visual pathway disorders (Fracasso et al., 2016a; Hoffmann et al., 2012). Last, ultra-high field MRI approaches extended beyond topographic organization to the identification of brain systems sub-serving higher order and complex cognitive functions such as an individual's perception of space, time, and people with respect to self (Peer et al., 2015).

However, not all analysis protocols will benefit from ultra-high field at conventional resolutions. In particular, use of spatial smoothing and/or averaging subjects in a common (linear) stereotaxic space (Collins et al., 1994; Talairach and Tournoux, 1988) will decrease the effective spatial resolution and thereby sacrifice the increased sensitivity and specificity. Ultra-high field MRI reinforces the need for alternatives to compare and align brains. Several methods are already developed amongst which, non-linear alignment in stereotaxic space and surface based alignments (Fischl et al., 1999; Gholipour et al., 2007; Klein et al., 2009). In that direction, ultra-high field MRI may inspire a new method of alignment by high-resolution anatomies based on myelin differences across cortical areas (Bridge and Clare, 2006; Deistung et al., 2013; Geyer et al., 2011). This will be further discussed in the sections below but delineating cortex based on myelin differences dates back a century ago to atlases of Vogt (Vogt and Vogt, 1919; Vogt, 1910) a contemporary of the more well-known Brodmann atlases (Brodmann, 1903, 1909).

Ultra-high field MRI at high spatial resolutions (< 1 mm): methodological considerations

To perform BOLD fMRI with high spatial (< 1 mm) and temporal resolution it is crucial to have sufficient sensitivity. The most effective way, albeit expensive, is to work at ultra-high field strength. As discussed above, going to ultra-high field strengths (≥7 T) provides a linear to supralinear increase in BOLD signal sensitivity. Other hardware approaches to increase BOLD sensitivity are to increase the numbers of receive channels or to employ dedicated surface receive coils (Petridou et al., 2012; Salomon et al., 2014; van der Zwaag et al., 2009b).

Besides hardware considerations, the specific physiological and biophysical sources of the BOLD signal strongly determine the response sensitivity and specificity, not only in amplitude but also in temporal behaviour. The larger venous vessels (intracortical, pial and large draining veins) have a large blood volume and are located furthest downstream resulting in higher amplitudes, more delayed and broader BOLD responses (blood pooling) that are the least specific to neuronal activity (de Zwart et al., 2005; Lee et al., 1995; Menon, 2002; Siero et al., 2011; Turner, 2002). BOLD signals from the microvasculature (arterioles, capillaries and small venules) have the highest spatial specificity to neuronal tissue and tend to show smaller amplitudes, faster and narrower responses with a notable heterogeneity across cortical depth (Jin and Kim, 2008; Ogawa et al., 1993; Siero et al., 2013; Siero et al., 2015; Silva et al., 2000; Tian et al., 2010; Uludağ et al., 2009; Yacoub et al., 2008; Yacoub et al., 2007; Yacoub et al., 2001).

The BOLD signal heterogeneity across the cortical depth becomes crucially important when pushing the spatial resolution to the domain of cortical laminae and columns – it contains depth-dependent variations in neuronal activity, but also non-neuronal related variations in vascular architecture, blood draining properties (Fig. 3) and other physiological noise components (Koopmans et al., 2011). These effects should be taken into account when analysing cortical-depth or laminar resolved fMRI (Gagnon et al., 2015; Goense et al., 2016; Heinzle et al., 2016; Kok et al., 2016; Markuerkiaga et al., 2016; Puckett et al., 2016).

The combined effect and spatial extent of the neuronal and non-neuronal related components of the BOLD signal can be described by a point-spread function (PSF). The PSF is expected to be 1) cortical depth dependent; because of pial and intracortical veins the PSF towards the surface is expected to be wider, potentially confounding laminar and columnar specificity (Markuerkiaga et al., 2016; Tian et al., 2010), 2) time dependent; because of blood pooling from deeper layers the PSF width can increase over time (Shmuel et al., 2007; Siero et al., 2013), 3) pulse sequence dependent; spin-echo BOLD PSF generally has a narrower width compared to a gradient-echo BOLD PSF (see gradient- and spin-echo BOLD discussed below, (Markuerkiaga et al., 2016; Parkes et al., 2005; Shmuel et al., 2007). Ultimately, the extent and width of the PSF determines the biophysical spatial resolution of BOLD fMRI.

The increased specificity of the ultra-high field fMRI signals is due to the increased sensitivity to microvasculature. As mentioned, with increasing field strength, the relative intravascular and extravascular BOLD signal contributions differ substantially. However, the amount of micro- versus macrovascular contributions to the fMRI signal depends also on the pulse sequence. Careful review of all these sequence details is beyond the scope of this review but we briefly want to highlight the major considerations for high-resolution fMRI (< 1mm).

Gradient-echo (GE, T2*-weighted) EPI based acquisition is currently the most popular method because of its superior sensitivity. However, this sensitivity comes at the cost of specificity due to the contributions of both the micro- and macrovasculature (Boxerman et al., 1995b; Ogawa et al., 1993). Exploiting the high spatial resolution, areas of large draining veins can be carefully removed to improve the spatial specificity to the parenchyma and thus aiding laminar or columnar resolved fMRI

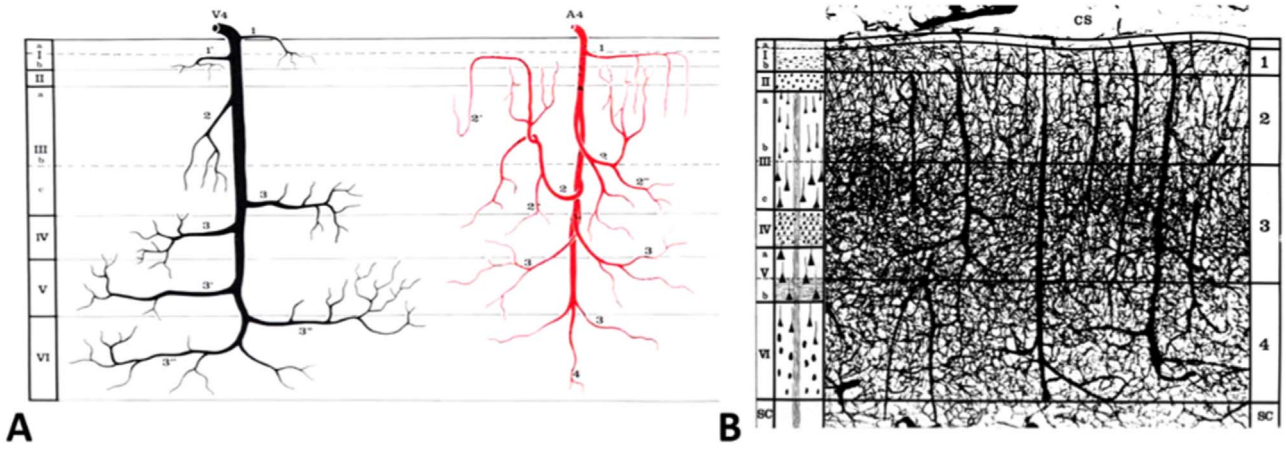

Fig. 3. Typical vascular organization across cortical depth in the cerebral cortex. A) Arteries and arterioles (in red) supply the neuronal layers, numbered I–VI from the cortical surface (CS) to the subcortical white matter (SC), with oxygen rich blood. In black are the venules and a principle intracortical vein oriented perpendicular to the cortical surface that can drain the blood from multiple functional units. B) Alongside the neuronal layers are the vascular layers 1–4 based on the orientation and density of the vessels (Reproduced from Duvernoy et al., 1981).

(Koopmans et al., 2010; Polimeni et al., 2010; Siero et al., 2014). However, this approach doesn't remove intra-cortical veins that penetrating the cortical surface. Furthermore, the effect of large draining veins at the pial surface can indirectly affect other layers (Markuerkiaga et al., 2016). This extravascular contamination declines with distance from the vessel - in the worst-case scenario it drops off by a factor of nine at a distance equal to the vessel diameter (Ogawa et al., 1993; Siero et al., 2011). From a neuroscience perspective, removing large draining veins decreases the ability to investigate signals at superficial cortical layers where most large veins are.

Spin-echo (T2-weighted) based acquisitions, have an increased microvascular weighting at ultra-high field, however at the price of reduced sensitivity, increased SAR, sensitivity to B1-inhomogeneity, and residual T2*-weighting in the case of long EPI readouts. Several types of T2-weighted based fMRI acquisitions have been explored at ultra-high field with a range of success; (segmented) 2D and 3D spin-echo EPI, 3D GRASE, SSFP, and T2 preparation pulses preceding a GE readout (Barth et al., 2010; De Martino et al., 2013; Goa et al., 2014; Harmer et al., 2012; Hua et al., 2014; Kemper et al., 2015; Sanchez Panchuelo et al., 2015; Yacoub et al., 2003).

Furthermore, cerebral blood flow (CBF) and blood volume (CBV) weighted acquisitions promise to have high microvascular weighting (Duong et al., 2002; Huber et al., 2015). Multi-modal imaging approaches that combine BOLD and CBF/CBV measurements may yield valuable cortical depth-dependent information on the neuronal and metabolic underpinnings of the BOLD response (Guidi et al., 2016; Huber et al., 2015). Lastly, with recent advances in fast scanning techniques, such as simultaneous multislice or multiband approaches, the temporal resolution of BOLD fMRI can be dramatically increased to subsecond sampling times (for a thorough overview see (Barth et al., 2016; Feinberg and Yacoub, 2012; Setsompop et al., 2016)). This will allow more accurate characterization of the BOLD fMRI temporal dynamics, information of which will greatly benefit BOLD signal modelling for high-resolution studies and may ultimately lead to laminar resolved connectivity measures.

Laminar imaging using ultra-high field MRI

Relevance of laminar imaging

Functional specialization is usually thought in terms of separate cortical areas serving specific computations, however this is not the only form of functional specialization that exists in human cortex. The layering across cortical depth represents an orthogonal dimension of functional specialization, separate from the different brain regions that can be observed at the macroscopic level. This type of organization is thought to gate the information flow between separate functionally specialized portions of the human cortex (Felleman and Van Essen, 1991; Rockland and Pandya, 1979a; Shipp, 2007). One of the ultimate promises of laminar analysis is that it can provide information on the direction of information flow in a given patch of cortex simply by comparing the relative contributions of different laminae (Fig. 4).

Historically, two different forms of layered cortical specialization have been described in the literature. From the structural perspective (i) several investigators began a systematic study of the human cortex since the beginning of the twentieth century, with the aim of parcellating human cortex into separate areas. These attempts took advantage of the layered organization of cytoarchitectonic features

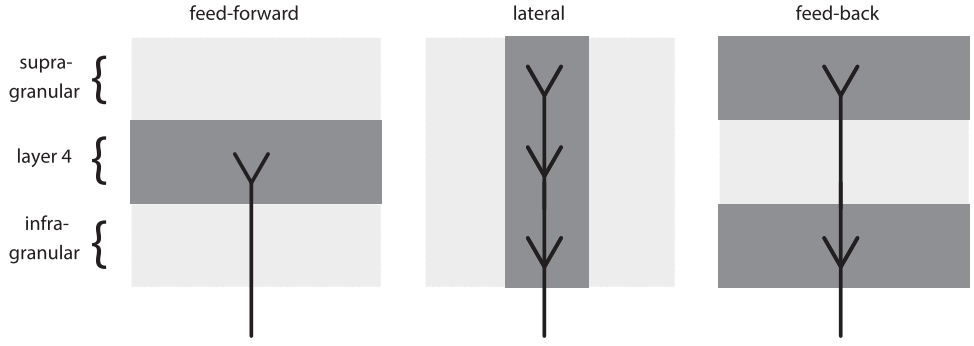

Fig. 4. Laminar patterns of cortical connectivity at their predominant termination sites (adapted from Felleman and Van Essen (1991)). These patterns were used for making hierarchical assignment of cortical areas showing feed-forward fibres arriving mainly in layer 4, lateral fibres targeting all three main compartments (infra-, layer 4, and supra-granular) indistinctively and feed-back fibres terminating in supra-granular and infra-granular layers.

(distribution of cell bodies and axons along cortical depth, (Brodmann, 1909; von Economo and Koskinas, 1925) and myeloarchitectonic features (distribution of myelin features along cortical depth, (Elliot Smith, 1907; Flechsig, 1901; Vogt and Vogt, 1919; Vogt, 1910)). On the other hand, from the functional perspective (ii), ascending (feed-forward) and descending (feedback) interactions within and between separate portions of cortex are segregated according to cortical depth (Felleman and Van Essen, 1991; Shipp, 2007). We will discuss the structural and functional contributions in turn.

Structural laminar organization in human cortex

The first observation suggesting a laminar organization in human cortex dates back in the eighteenth century, when Francesco Gennari, reported the presence of a prominent line located approximately in the middle of the cortical thickness, at the level of the calcarine fissure (Gennari, 1782). This is the origin of the widely used distinction between striate and extrastriate cortex. Today we know that the Stria of Gennari is a band of highly myelinated fibres, located at the granular layer, where heavily myelinated thalamo-cortical afferents reach primary visual cortex (V1). Less than a century after Gennari's observation, leading researchers became to believe that a laminar organization was not only confined to the calcarine fissure. In 1840, Jules Baillarger reported the existence of two separate bands of white fibres, running throughout the cortex (Baillarger, 1840). The bands of Baillarger consist of two bundles of myelinated fibres, located in the internal granular layer of layer IV and internal pyramidal layer of layer V. At the beginning of the twentieth century several investigators started a systematic study of the human cytoarchitectonic (Brodmann, 1909; von Economo and Koskinas, 1925; Zilles and Amunts, 2010; Zilles et al., 2004) and myeloarchitectonic features across cortical depth (Campbell, 1905; Elliot Smith, 1907; Kaes, 1907; Vogt and Vogt, 1919; Vogt, 1910), with the aim of parcellating human cortex into separate areas, isolating several portions of the cortex based on their structural features, hoping to be able to clarify their functional counter-aspect in the future.

Although the underlying cytoarchitectonic features cannot be directly investigated, the myeloarchitectonic features are within reach using MRI. Although myelin represents the main source of contrast in structural (T1-weighted) images, MRI is an indirect measure of myelin. The main goal of these studies is to reveal intra-cortical laminar structures. Several attempts have been made to visualize intra-cortical laminar patterns in-vivo, at different spatial scales. Human cortex is cortical thickness ranges between 1 and 4 mm (Fischl and Dale, 2000), thus to allow accurate visualization of intra-cortical details sub-millimetre resolution data with high signal-to-noise ratio (SNR) are crucial.

Several studies visualized detailed intra-cortical laminar patterns within the human primary visual cortex, visualizing the Stria of Gennari that defines primary visual or striate cortex (Barbier et al., 2002; Bridge et al., 2005; Eickhoff et al., 2005; Fracasso et al., 2016c; Trampel et al., 2011) (Fig. 5a and b). Furthermore, intra-cortical details were observed in locations outside primary visual cortex (Sanchez-Panchuelo et al., 2012), and in motion-sensitive area MT or V5 (Walters et al., 2003). Recently, the presence of laminar intra-cortical features has been reported in vivo at the level of the calcarine cortex (the Stria of Gennari) as well as in extra-calcarine areas, extending to parietal and frontal lobes with data acquired at 0.5mm isotropic resolution (Fracasso et al., 2016c). This feature outside primary visual cortex likely represents the bands of Baillarger. Moreover, detailed myelin profiles have been reported in vivo from area BA1, BA4 and BA3b from T1 maps acquired at 0.5mm isotropic at 7 T, using a volume-preserving model to compute the metric across cortical depth (Waehnert et al., 2016; Waehnert et al., 2014).

At a macroscopic level, these myelination patterns have been used to effectively identify a large number of cortical areas, matching probabilistic atlases based on cytoarchitectonic data as well as retinotopic and auditory maps (Bock et al., 2013; De Martino et al., 2014; Dick et al., 2012; Fischl et al., 2008; Geyer, 2013; Geyer et al., 2011; Glasser and Van Essen, 2011; Hinds et al., 2008; Lutti et al., 2014; Marques and Gruetter, 2013; Sanchez-Panchuelo et al., 2012; Sereno et al., 2013; Tardif et al., 2015). Being able to detect the presence of these features might provide the basis for the in vivo parcellation of human cortex, a quest also referred to as “in vivo histology” (Bridge and Clare, 2006; Deistung et al., 2013; Geyer et al., 2011), enabling researchers to elaborate detailed hypotheses on the relationships between structure and function in the human brain.

Functional laminar organization in human cortex

One of the first studies to investigate the functional significance of the laminar differentiation of the cerebral cortex goes back to Clark and Sunderland (1939) who isolated a small portion of primary visual cortex in macaque from neighbouring gray matter locations, while keeping intact their contact with the white matter and the pial vessels irrigating the isolated cortex. Their aim was to study the laminar pattern of degenerating fibres after prolonged isolation. In these conditions the isolated cortex remained remarkably unaltered for as long as 3 months after surgery, and indicates the abundance of intracortical connexions with directly neighbouring cortex. Visible changes could be observed only at the level of the infra-granular layers, whereas the Stria of Gennari remained unaltered.

Hubel and Wiesel studied the laminar and columnar organization of the geniculo-cortical pathway in a series of papers (Hubel and Wiesel, 1968; Hubel and Wiesel, 1972; Hubel and Wiesel, 1977) and reported clear evidence suggesting that layer IV in monkey primary visual cortex represents the major (but not the only (Sincich and Horton, 2005)) afferent location for the geniculo-cortical pathway. Later, Tigges and colleagues (Tigges et al., 1977) reported that feedback projections from area V2 to V1 tended to avoid the location occupied by the geniculo-cortical pathway in primary visual cortex. This latter observation was rapidly generalized also to connections between other occipital visual areas (Graham et al., 1979; Rockland and Pandya, 1979b; Wong-Riley, 1979), following a similar pattern as the one observed in primary visual cortex, with feed-forward fibres arriving mainly in layer 4, feed-back fibers terminating in supra-granular and infra-granular layers and lateral fibres targeting all three main compartments (infra-, granular and supra-granular) indistinctively (Fig. 4). This pattern of fibre termination was later adopted for the hierarchical assignment of cortical areas (Felleman and Van Essen, 1991). The six separate cortical layers are not directly resolved using MRI and, hence, the signals are typically described as depth-dependent or by the more coarse granular terminology.

Several recent studies investigated laminar variations of the fMRI signal (Fig. 5b and c), focusing on the underlying neurovascular coupling in humans (Chen et al., 2012; De Martino et al., 2013; Huber et al., 2014; Huber et al., 2015; Koopmans et al., 2010; Koopmans et al., 2011; Olman et al., 2012; Polimeni et al., 2010; Ress et al., 2007; Siero et al., 2011) and non-human primates (Goense et al., 2012; Goense and Logothetis, 2006; Goense et al., 2007) as well as other mammals (Harel et al., 2006; Jin and Kim, 2008; Silva et al., 2000). Cortical depth-dependent studies in humans and animals (Chen et al., 2012; De Martino et al., 2013b; Goense et al., 2012) using gradient echo EPI consistently demonstrate an increase in signal change towards the pial surface in the human cortex reflecting the cortical vascular organization and blood pooling towards the pial surface (Chen et al., 2012; De Martino et al., 2013; Fracasso et al., 2016b; Goense et al., 2012). Attempts have been made to increase the spatial specificity of the BOLD signal towards the capillary bed by moving towards spin-echo (Goense et al., 2007) and, more recently, 3D GRASE sequences (De Martino et al., 2013). Evidence from animal studies shows that cerebral blood volume (CBV) changes across cortical depth peak in locations closer to the site of changes in metabolic

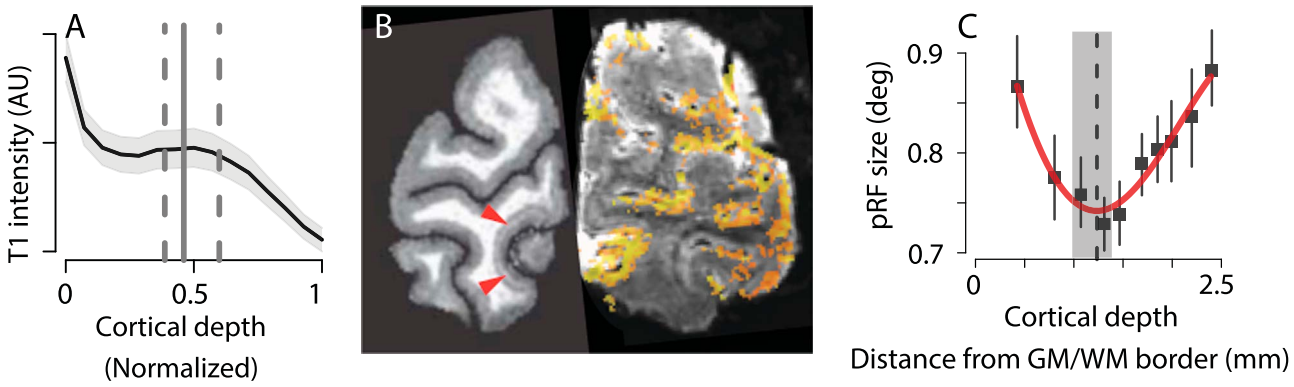

Fig. 5. Structural and functional laminar imaging. A) Average T1 intensity across cortical depth from V1 (6 participants). Vertical continuous and dashed lines represent the median and 95% CI of the peak estimate, indicating the location of the stria of Gennari approximately in the middle of cortical depth, the location where heavily myelinated thalamo-cortical afferents reach V1. B) 0.5 mm isotropic T1-weighted (T1-w) and T2*-weighted, 3D-EPI images from the occipital lobe, juxtaposed. Red arrows on the T1-w image indicate the prominent Stria of Gennari (Fracasso et al., 2016c). The overlay on the 3D-EPI image represents the activity in response to full field visual stimuli ($T > 2$, $p < 0.05$, uncorrected). C) The relationship between population receptive field (pRF) size and distance from white matter border. PRF size estimates follow a U-shaped function, with larger pRF sizes close to the white matter border and the pial surface, as expected based on the thalamo-cortical afferents reaching V1 and the hierarchical signal processing within the cortical sheet (Fracasso et al., 2016b). Vertical solid and dashed lines and shaded region represent the median location of the profile minimum and 95% CI.

activity (Goense et al., 2007; Kennerley et al., 2005; Kim et al., 2013). It has been recently reported that it is possible to measure cerebral blood volume (CBV) in humans, non-invasively (Huber et al., 2014; Lu et al., 2013) showing lower sensitivity to the macrovasculature compared to gradient-echo BOLD (at 7 T) and higher specificity to changes at the microvasculature level.

Sub-millimeter functional imaging studies has also reached several neuroscience applications. The vascular influence, in particular the changing sensitivity or signal amplitude across cortical depth, complicates neuroscientific studies as mentioned previously. These are partly relieved by the aforementioned sequence developments, but, in addition, computational neuroimaging approaches can help overcome the problem as well. Certain computational designs depend less on signal amplitude. Although, of course, a certain amount of signal needs to be present but, once enough signal is present, signal increases do not further determine the outcome of the analysis. Example of computational analyses employed are multivoxel pattern classification techniques (Muckli et al., 2015), population receptive field (pRF) (Fracasso et al., 2016b) and population tuning analyses (De Martino et al., 2015). De Martino and colleagues showed that attention sharpens the responses specifically in supra-granular layers of the temporal cortex, whereas Fracasso and colleagues demonstrated that pRF sizes vary systematically across cortical depth in a manner that resembles the hierarchical information flow through the cortex (Fig. 5c). In an excellent example of the application of laminar fMRI in neuroscience, Kok and colleagues studied the response of primary visual cortex to the famous illusory Kanizsa triangle (Kok et al., 2016). The authors showed that feedback activity associated with illusory contours is associated with a selective activation of the deeper layers. The study further demonstrates the feasibility to isolate feedback activity in-vivo in humans.

To summarize, laminar or cortical depth dependent imaging at ultra-high field will help to bridge the gap between neurophysiology and functional imaging, opens the possibility of delineation of cortical areas by structural laminar imaging and draw inference about the direction of information flow in the brain using functional laminar imaging.

Columnar imaging at ultra-high field MRI

Relevance of columnar imaging

The ability and potential of non-invasive imaging of cortical columns is a much-desired application of ultra-high field functional MRI. In a cortical column, neurons with similar functional or computational properties are grouped together vertically across cortical depth. The neuron's response profiles across the column are similar but not identical as the column itself is split into laminae with different input and output relationships. Different columns are thought to represent the different computations an area performs, such as orientation and ocular dominance columns in primary visual cortex. Besides columnar organisation within an area, between area connections are often columnar (Goldman and Nauta, 1977; Jones et al., 1975). In primary visual cortex, different columnar structures are organized in such a way that all combinations repeat themselves – the basis of the notion of a hypercolumn or cortical computational unit (Fig. 1).

Cortical columns were first discovered by Mountcastle in cat somatosensory cortex (Mountcastle et al., 1955; Mountcastle, 1957). Mountcastle used vertical penetrations of electrodes and found that vertical clusters of cells that responded to a specific somatosensory stimulation (e.g. skin, joint) were organized in a modular fashion that varied periodically across the cortex, in steps of about 500 μm. This work was succeeded by Hubel & Wiesel, who identified orientation and ocular dominance columns in cat and monkey visual cortex (Hubel and Wiesel, 1962, 1963, 1968, 1969). Since then, several studies using electrophysiological, optical and anatomical manipulations have identified columnar organization across several species, including humans, with the majority of work focussing on visual cortex.

An intriguing observation in these studies is that columns are not universal across species. For example, ocular dominance columns are present in the ferret, mink, marmoset, baboon and several primates including humans. They are absent in the rat, mouse, squirrel, rabbit, and other species (reviewed in (Horton and Hocking, 1996)). Moreover, even within the same species, some individuals have ocular dominance columns while others not, or only in parts of primary visual cortex (Adams and Horton, 2003). Similarly, orientation columns are found in many species, e.g. monkey, cat and human, while they appear to be absent in others, e.g. mice and rats. However, no specific differences in vision or visual perception have been found between and within species, raising the question of the necessity of columnar organization for function (Horton and Adams, 2005).

Of particular relevance for fMRI, relating to the expected signal changes and spatial patterns obtained, is that columns generally do not have distinct borders but are rather comprised by a “core” set of neurons with the same functional properties, surrounded by neurons that share functional properties with neighbouring columns. Therefore, the spatial pattern of activity of neighbouring columns as detected by fMRI is expected to partially overlap not only because of the presumably wider spatial point-spread function of the hemodynamic response with respect to column width, but also because of the neuronal activity pattern within a column and neuronal communications between columns (Gilbert and Wiesel, 1983; Rockland and Lund, 1982).

Because neurons with similar response properties organize themselves in columns, columnar responses as a whole can provide information about the fundamental processing of the individual neurons. This is the ultimate goal of columnar imaging. We hypothesize that columnar structures may be found throughout the brain and may not only play a role in within area organisation but also in connectivity between areas. This hypothesis may or may not be prove to be true. Regardless, columnar imaging using ultra-high resolution fMRI may elucidate the role of columns and their presence or absence in brain organisation and function. Even though, the notion of a cortical computational unit is linked to the observation of multiple columns, it does not, strictly speaking, depend on the presence of columns, as we interpret it as a functional neuronal organization unit that repeats itself across an area. If an area proves not to contain columnar structures the question remains what the organization principles are for the underlying neurons. Therefore, the ability to image and measure from columns can give us insights into brain function and circuitry at that fundamental level, considerably fostering our understanding of brain organization from single neurons to brain systems.

Columnar organization in human cortex

In vivo and in humans, (f)MRI is in essence the only technique that can be used to image columns because it is non-invasive and because of the high resolution it affords especially at high magnetic fields. A downside is that fMRI measures hemodynamics and not neuronal activity directly, therefore a key question is whether hemodynamics are specific enough to the underlying neuronal patterns to be able to accurately resolve columnar organization. This has been the key question for the majority of hemodynamic-based studies on columnar organization to date.

Early optical imaging studies demonstrated that hemodynamics do indeed have the specificity to resolve cortical columns (Bonhoeffer and Grinvald, 1991; Grinvald et al., 1986; Ts'o et al., 1990). In later work, it was shown that the early deoxygenation concomitant with an increase in neuronal metabolism (“initial dip”), and early hyperoxygenation in the microvasculature have the highest specificity to cortical columns, while delayed blood volume and blood flow are less specific (Grinvald et al., 2000; Malonek and Grinvald, 1996). However, if one minimizes the contribution of larger vessels, for example using a differential approach (contrasting one stimulus condition to another), it emerges that the micro-vascular blood flow and volume are also specific to cortical columns (Vanzetta et al., 2004; Wang and Roe, 2012). These findings suggest a fine regulation of the micro-vascular response that co-localizes with columns (Woolsey et al., 1996) although alternative explanations also exist (Blinder et al., 2013). Nevertheless, translation of optical imaging findings to fMRI is not straightforward given that the techniques have different resolutions, different sensitivity, and may measure from different parts of the vasculature since optical imaging studies primarily measured from the upper cortical layers due to limited light penetration.

Kim and colleagues undertook the challenge of translating and extending optical imaging findings to MRI, providing a detailed account of fMRI sensitivity and specificity to columnar organization based on the well-established orientation column model in cat visual cortex (Duong et al., 2001; Fukuda et al., 2006; Kim et al., 2000; Moon et al., 2007; Zhao et al., 2005). A common methodological aspect for all their studies was the use of high field (4 T and/or 9.4 T) with small surface coils to ensure high SNR for high-resolution imaging (in plane resolution 0.15×0.15 mm or 0.31×0.31 mm, slice thickness 1 or 2mm). A second methodological aspect was the selection of a single slice positioned in order to avoid the pial surface and ensure minimal contribution from larger vessels that can reduce fMRI specificity. Encouragingly, their work demonstrated that roughly all aspects of the hemodynamic response measured with MRI have the specificity to accurately resolve columnar organization, ranging from the initial dip (representing an early increase in CMRO2; (Kim et al., 2000)), blood flow (CBF; (Duong et al., 2001)), blood volume (CBV, (Fukuda et al., 2006; Zhao et al., 2005)), and the positive BOLD measured with spin-echo and gradient-echo EPI (Moon et al., 2007). Notably, the sensitivity of each contrast and technique above is almost reversed in the same order, with the exception of a high sensitivity for CBV, which was acquired with a monocrystalline iron oxide nanoparticle (MION) contrast agent, which cannot be used in humans. The work by Moon et al. (2007) is particularly encouraging for human applications since the positive BOLD is the most commonly used contrast in humans because of its high sensitivity.

Stimulation paradigm also affects the ability to visualize cortical columns, i.e. differential approaches, single condition (active vs baseline), and continuous stimulation (Grinvald et al., 2000; Kim et al., 2000; Kim and Ogawa, 2012; Moon et al., 2013; Moon et al., 2007). A differential approach is beneficial because it can minimize the contribution of larger veins but it is contingent on stimuli that are orthogonal to each other (e.g. left vs right eye) such that they can be effectively subtracted. However, even in the case that such stimuli can be designed, signals from draining veins may be stimulus-specific. This is nicely demonstrated in the work by Shmuel et al. (2010), who showed that signals from draining veins can be used to decode which eye was stimulated (implying ocular dominance selectivity), albeit at a coarser spatial scale than columns. A single condition on the other hand is beneficial because it does not necessitate orthogonal stimuli, and therefore applicable for columns possibly underlying higher order brain functions. However, such a design will be more susceptible to the point-spread of the hemodynamic response and signals from larger veins. Continuous stimulation can mitigate hemodynamic “artifacts” by saturating large draining veins (standard approach for topographic and pRF mapping), although it requires a continuous stimulus space and the direct or indirect characterization of responses using neuronal tuning curves or biologically-inspired models.

In humans, earlier studies primarily focused on the feasibility of positive BOLD fMRI to map ocular dominance columns in primary visual cortex, tackling the issues of large draining veins, subject motion, and sufficient SNR for high-resolution imaging. A highlight from all human studies is that SNR and subject motion are crucial issues in imaging columns in humans. All but one studies have employed surface coils or custom coils to enhance SNR for high resolution, even at 7 T. In most cases a single or few slices were acquired, balancing high in-plane spatial resolution and imaging speed. As acquisition schemes evolved, coverage increased to larger parts of cortex with isotropic spatial resolutions which are suitable for convoluted cortex unlike single or few anisotropic slices. Moreover, almost all studies have employed strict head immobilization approaches such as bite-bars or mechanical support because even very small movement can be detrimental for the detection of columns. For instance, the width of ocular dominance columns in human primary visual cortex is about 850 μm (Adams et al., 2007) imposing strict criteria for acceptable head motion, i.e. below 1 mm.

On the path of feasibility, Menon and colleagues were the first to tackle the feasibility of mapping ocular dominance columns at 4 T using gradient-echo FLASH and exclusion of larger veins using a differential approach and thresholding voxels with high signal changes corresponding to large pial veins (Menon et al., 1997). Dechent and Frahm (Dechent and Frahm, 2000) also suggested the feasibility of mapping ocular dominance columns using FLASH at 2 T. In subsequent work, Menon and Goodyear suggested that ocular dominance columns could be mapped more robustly by avoiding large draining veins using short stimuli (Goodyear and Menon, 2001) and utilizing the early part of the BOLD response (Menon and Goodyear, 1999). However, a common criticism of the work of Menon and colleagues was that the ocular dominance columns appear to extend beyond primary visual cortex and it is well known they terminate at the border of primary visual cortex. The question was whether they resolved biases in eye dominance versus the actual ocular dominance per se. Cheng et al. (Cheng et al., 2001) adopted

a different approach, also at 4 T, and demonstrated robust detection of ocular dominance columns using long stimulus duration but also accounting for large draining veins with careful slice positioning, differential mapping, and thresholding of voxels corresponding to large pial veins. Importantly, Cheng et al. focussed on the border of primary visual cortex, which allowed a direct comparison of regions known to contain ocular dominance columns with those known not to contain them. Furthermore, because of the known ocular dominance column orientation at the border, this study provided the first well accepted evidence of locating ocular dominance columns in humans. With the advent of 7 T scanners, where the use of spin-echo became meaningful due to reduced intra-vascular signals and increased SNR, Yacoub and colleagues (Yacoub et al., 2007) demonstrated that large vein signals are significantly reduced in spin-echo as compared to gradient echo ocular dominance maps, indicating that spin-echo imaging would more appropriate for single condition approaches, although both spin-echo and gradient-echo maps were highly robust.

Later work moved to more challenging domains, providing the first in vivo demonstration of orientation columns in human primary visual cortex (Yacoub et al., 2008) (Fig. 6a and b), and the first in vivo demonstration of axis-of-motion columnar organization in human MT (Zimmermann et al., 2011). Still largely focused on feasibility, the later study showcased advantages in methodology that can greatly facilitate imaging of columnar structures, particularly the use of 3D fMRI (3D GRASE) with isotropic spatial resolution, thus enabling imaging of convoluted cortex, and enabling the use of laminar segmentation and surface rendering tools to visualize the patterns in 3D and across cortical depth. This is an advantage for two reasons, first because maps can be examined at a distance from the pial surface, and second because the pattern of columns can be visualized and characterized across cortical depth.

Recent studies have ventured into neuroscientific questions focusing on less well-charted functional domains, highlighting the potential of ultra-high field fMRI to provide new insights on human brain organization. From a methodological point of view, the issue of large draining veins in the studies below appears settled either with the use of hybrid spin-echo acquisitions (3D GRASE) or by avoiding the pial surface for gradient-echo EPI. Sun et al. (2007) identified a previously unknown column-like organization in primary visual cortex (V1) consisting of clusters of neurons tuned to the temporal frequency of visual stimuli, providing new knowledge on how neurons are organized in response to stimulus properties and on how visual information is processed in human V1. Zhang et al. (2010) demonstrated that fMRI can resolve excitatory and inhibitory processes at the level of ocular dominance columns, employing a novel paradigm design manipulating the binocular interaction between ocular dominance columns, paving the way to study brain circuits and dynamic local processing at the level of fundamental cortical processing units. Dumoulin et al. (2013) and Nasr et al. (2016) probed column-like organization in visual areas V2 and V3, structures known as stripes because of their stripe like appearance in histological manipulations (Fig. 6c and d). Neurons in these stripes process different features of the visual scene such as color or motion, and are considered to play a key role in the increasing functional specialization across visual areas. Their existence in V2 was known from invasive measurements in monkeys, while their existence in V3 was unclear. These studies provided in vivo evidence of the presence of stripes in human V2 and V3. Notably Nasr et al. (2016) also presented ocular dominance maps on the inflated cortical surface based on signals acquired away from pial veins, extending previous work from limited slices to larger brain coverage at isotropic resolution, exemplifying again the potential of recent advances in data acquisition and processing to facilitate columnar imaging (Fig. 6c). Further, selective cortical structures resembling columns are suggested in neighbouring visual areas supporting the neuronal computations that underlie depth perception (Goncalves et al., 2015). Lastly, De Martino et al. (2015) ventured outside visual cortex to auditory cortex, suggesting a column-based organization of frequency tuned neurons across cortical depth, paving the way to decipher the role of columns in auditory cortical processing.

In summary, imaging columns remains a great challenge but with the combination of increasingly evolving ultra-high field technologies, acquisition methods, data processing tools, experiment designs, and also increasing confidence in the accuracy of the signals measured, we may see a boost in the application of functional MRI to explore columnar organization in the human brain.

Conclusions

Ultra-high field MRI provides several advantages and challenges for systems neuroscience. First and foremost, the increased magnetization provides an increased sensitivity and specificity that will benefit most MRI studies. For conventional spatial resolution functional imaging (> 1 mm) ultra-high field appears sufficiently matured and the enhanced signal-to-noise and sensitivity are being capitalized to explore brain organization and functions in a new light. Second, ultra-high field MRI provides measurements on a fine organization scale of the human brain, i.e. the mesoscopic scale where laminar and columnar features arise. From a structural MRI perspective, ultra-high field may be able to delineate brain areas based on in vivo histology (Deistung et al., 2013). Laminar organization may provide an important new direction

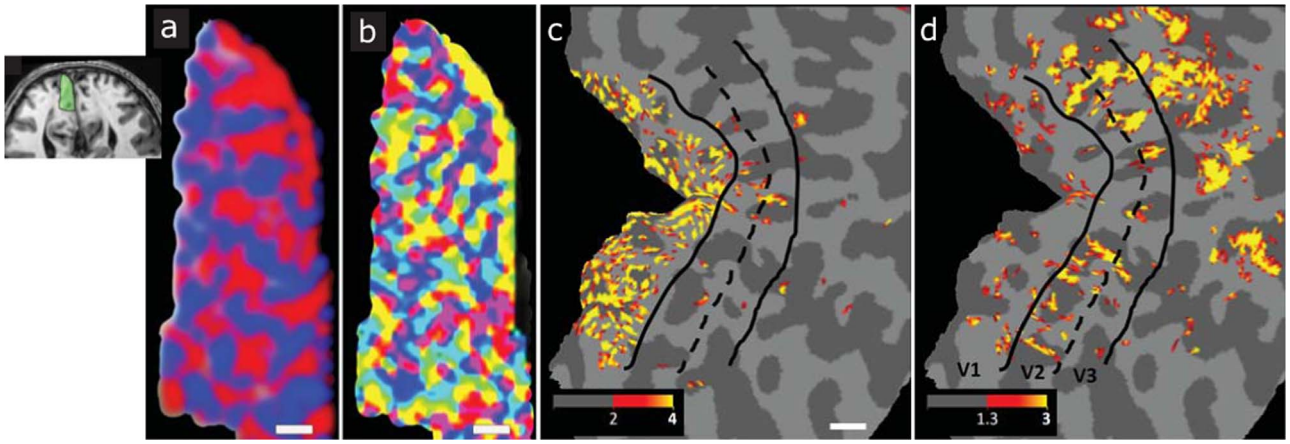

Fig. 6. Ocular dominance (a) and orientation (b) column maps in the same part of V1 of one subject (adapted from Yacoub et al., 2008), scale bar 1 mm). In this work Yacoub and colleagues used a single slice positioned on a flat part of the calcarine sulcus (marked green in the inset). The pattern of ocular dominance columns, contrasting binocular versus monocular stimulation, projected on the inflated cortical surface for one subject (c). The black lines mark the borders between V1, V2, and V3 (see d). Occular dominance columns end at the V1/V2 border. In V2 and V3 a stripe organization emerges (d) (adapted from (Nasr et al., 2016), scale bar 1 cm).

for fMRI, potentially allowing the direction of information flow to be deciphered from high-resolution MRI, not by the temporal component but by the layer component, whereas columnar organization may indicate the fundamental computations performed in a given area.

The potential impact of the columnar organization is that the column reflects the features of the individual neurons within the column. As such, columnar imaging holds the promise to reveal the fundamental computations performed by a given cortical area. Columns are well-established features of primary visual cortex, though admittedly only in certain species, including humans. Columns have also been demonstrated in primary somatosensory and motor cortex and similar organization features are suggested for auditory cortex (De Martino et al., 2015). We hypothesize that this columnar organization and the notion of a cortical computational unit extends further to other brain regions as well. The visual system currently provides the gold standard for high-resolution fMRI protocols to reveal columnar and laminar structures. We know where the columns are and where they terminate. Once we can reliably detect these features of the visual system, we can turn our attention to more unexplored regions of cortex. Higher-order brain regions pose yet another challenge, particularly for columnar investigations: which task and analysis to use is unclear, given that very limited insights exist from invasive animal work. Promising experiments at regular resolutions, however, provide evidence that at least some of the (topographic) principles of sensory and motor cortices extend to the field of numerical cognition (Harvey et al., 2015; Harvey et al., 2013) and language (Huth et al., 2016). In summary, we propose that columns reflect the fundamental neuronal computations of a given area and that ultra-high field MRI will be a critical tool for neuroscientists to visualize signals at the columnar level in living humans. In summary, we propose that columns reflect the fundamental neuronal computations of a given area (Mountcastle, 1978; Rockel et al., 1980) and that ultra-high field MRI will be a critical tool for neuroscientists to visualize signals at the columnar level in living humans.

The impact we describe of high-resolution ultra-high field MRI involves predominantly basic scientific insights into the fundamental operations of the brain. However, we envision that these insights will also translate to clinical neuroscience. We speculate that the cortical processing unit and its columnar and laminar components may be altered in certain clinical conditions reflecting the altered computations. For example, current hypotheses propose that in congenital visual pathway disorders the columnar structures are altered (for review see (Hoffmann and Dumoulin, 2015). Specifically, because the connections between the eyes and the brain are altered the proposal is that in some subset of conditions the ocular dominance columns are replaced by – or perhaps recycled into – hemifield columns. This hypothesis is in part guided by the suggestion from animal models that in one particular visual pathway condition (achiasma) the normally layered ocular structure of subcortical nuclei are replaced by hemifield layers (Williams et al., 1994). If this hypothesis proves correct, it would indicate that (1) columnar structures may be altered to reflect the altered computations of the diseased brain and (2) columnar structures may be preserved suggesting the relative importance in the cortical computational unit. Regardless of the outcome, in humans these questions can currently only be addressed using ultra-high field MRI.

Despite these exciting promises of ultra-high field MRI, there are several major methodological challenges that need to be addressed. No standard protocols exist that can reliably image laminar and columnar structures in every subject, limiting widespread neuroscience and clinical applications. For laminar and columnar imaging that typically require resolutions below 1mm, signal-to-noise and sensitivity remain a challenge, specifically for fMRI. An additional challenge is the balance between high spatial and temporal resolution; very high spatial resolution (< 1 mm) typically comes at the cost of low temporal resolution which translates to slow sampling of the hemodynamic response and likely loss of functional specificity and prolonged scan times. The latter can be a burden for the subject but also increases the chances of artifacts due to subject motion. Signal-to-noise and sensitivity is commonly enhanced with the use of surface coils, at the cost of reduced coverage. Whole brain imaging likely requires new approaches in coil designs that can extend the advantages of surface coil designs to whole brain coverage. The combination with increasing developments in accelerated imaging that exploit the coil geometry offers an avenue to increase the temporal resolution for very high spatial resolution fMRI (Setsompop et al., 2016), hopefully extending to whole brain imaging with new hardware technologies. Another important consideration is specificity. Although we have witnessed considerable progress in acquisition and analysis approaches that enable targeting the micro-vascular component that is specific to neuronal activity, it is still unclear how much of the fMRI signal measured reflects vascular or neuronal signals. For example, it is still unclear how vascular responses pool across cortical depth, either linearly or non-linearly, and how best to account for this in the data-analysis. Specificity could be improved with a better understanding of the hemodynamic point-spread function across cortical depth and vascular compartments, but also of the relationship to neuronal activity features which are complex on their own. This task may be within reach in well-described primary cortices but certainly a challenge in higher order brain regions that are not well characterized. Last, conventional data-analysis approaches in the neuroimaging field are not suitable for ultra-high field MRI, for example common use of spatial smoothing and averaging subjects in a common (linear) stereotaxic space will remove the enhanced spatial resolution and benefits of ultra-high field MRI. Thus the advent of ultra-high field MRI requires both a new set of data-acquisition techniques as well as new data-analysis techniques.

In this review, we speculate that the mesoscopic organization level contains a collection of neurons that together form the basic cortical computation unit of the brain. This is a concept derived from the hypercolumn notion (Hubel and Wiesel, 1977) and we have previously demonstrated evidence using 3 T MRI that this computational unit is roughly constant sized across primary visual cortex (Harvey and Dumoulin, 2011). This analysis was based on the relationship of secondary features, such as cortical magnification and population receptive field sizes, but ultra-high field MRI provides the promise to visualize the cortical processing unit and it's laminar and columnar components directly not only in primary visual cortex but throughout the entire human cortex.

Acknowledgements

This work has supported by the European Union's Horizon 2020 research and innovation programme under the Marie Sklodowska-Curie grant agreement No 641805 (S.D.), Ammodo KNAW Award (S.D.) and a Netherlands Organization for Scientific Research (NWO) Vidi Grant 13339 (N.P.). The Spinoza Centre is a joint initiative of the University of Amsterdam, Academic Medical Center, VU University, VU University Medical Center, Netherlands Institute for Neuroscience and the Royal Netherlands Academy of Sciences.

References

Adams, D.L., Horton, J.C., 2003. Capricious expression of cortical columns in the primate brain. Nat. Neurosci. 6, 113–114.
Adams, D.L., Sincich, L.C., Horton, J.C., 2007. Complete pattern of ocular dominance columns in human primary visual cortex. J. Neurosci. 27, 10391–10403.
Baillarger, J.G.F., 1840. Recherches sur la structure de la couche corticale des circonvolutions du cerveau. Mem. Acad. R Med. 8, 149–183.
Barbier, E.L., Marrett, S., Danek, A., Vortmeyer, A., van Gelderen, P., Duyn, J., Bandettini, P., Grafman, J., Koretskyk, A.P., 2002. Imaging cortical anatomy by high-resolution MR at 3.0T: detection of the stripe of Gennari in visual area 17. Magn. Reson. Med. 48, 735–738.
Barendregt, M., Harvey, B.M., Rokers, B., Dumoulin, S.O., 2015. Transformation from a retinal to a cyclopean representation in human visual cortex. Curr. Biol. 25, 1982–1987.
Barth, M., Breuer, F., Koopmans, P.J., Norris, D.G., Poser, B.A., 2016. Simultaneous

multislice (SMS) imaging techniques. Magn. Reson. Med. 75, 63–81.
Barth, M., Meyer, H., Kannengiesser, S.A.R., Polimeni, J.R., Wald, L.L., Norris, D.G., 2010. T2-weighted 3D fMRI using S2-SSFP at 7 T. Magn. Reson. Med. 63, 1015–1020.
Beckett, A., Peirce, J.W., Sanchez-Panchuelo, R.M., Francis, S., Schluppeck, D., 2012. Contribution of large scale biases in decoding of direction-of-motion from high-resolution fMRI data in human early visual cortex. Neuroimage 63, 1623–1632.
Blinder, P., Tsai, P.S., Kaufhold, J.P., Knutsen, P.M., Suhl, H., Kleinfeld, D., 2013. The cortical angiome: an interconnected vascular network with noncolumnar patterns of blood flow. Nat. Neurosci. 16, 889–897.
Bock, N.A., Hashim, E., Janik, R., Konyer, N.B., Weiss, M., Stanisz, G.J., Turner, R., Geyer, S., 2013. Optimizing T1-weighted imaging of cortical myelin content at 3.0 T. Neuroimage 65, 1–12.
Bonhoeffer, T., Grinvald, A., 1991. Iso-orientation domains in cat visual cortex are arranged in pinwheel-like patterns. Nature 353, 429–431.
Boxerman, J.L., Bandettini, P.A., Kwong, K.K., Baker, J.R., Davis, T.L., Rosen, B.R., Weisskoff, R.M., 1995a. The intravascular contribution to fMRI signal change: monte Carlo modeling and diffusion-weighted studies in vivo. Magn. Reson. Med. 34, 4–10.
Boxerman, J.L., Hamberg, L.M., Rosen, B.R., Weisskoff, R.M., 1995b. Mr contrast due to intravascular magnetic-susceptibility perturbations. Magn. Reson. Med. 34, 555–566.
Bridge, H., Clare, S., 2006. High-resolution MRI: in vivo histology? Philos. Trans. R Soc. Lond. B Biol. Sci. 361, 137–146.
Bridge, H., Clare, S., Jenkinson, M., Jezzard, P., Parker, A.J., Matthews, P.M., 2005. Independent anatomical and functional measures of the V1/V2 boundary in human visual cortex. J. Vis. 5, 93–102.
Brodmann, K., 1903. Beiträge zur histologischen Lokalisation der Grosshirnrinde. II. Der Calcarinustyp. J Psychol. Neurol. II, 133–159.
Brodmann, K., 1909. Vergleichende Lokalisationslehre der Großhirnrinde in ihren Prinzipien dargestellt auf Grund des Zellenbaues. Barth, Leipzig.
Campbell, A.W., 1905. Histological Studies on the Localization of Cerebral Function.
Chen, G., Wang, F., Gore, J.C., Roe, A.W., 2012. Identification of cortical lamination in awake monkeys by high resolution magnetic resonance imaging. Neuroimage 59, 3441–3449.
Cheng, K., Waggoner, R.A., Tanaka, K., 2001. Human ocular dominance columns as revealed by high-field functional magnetic resonance imaging. Neuron 32, 359–374.
Collins, D.L., Neelin, P., Peters, T.M., Evans, A.C., 1994. Automatic 3D intersubject registration of MR volumetric data in standardized Talairach space. J. Comput. Assist Tomogr. 18, 192–205.
Da Costa, S., van der Zwaag, W., Marques, J.P., Frackowiak, R.S., Clarke, S., Saenz, M., 2011. Human primary auditory cortex follows the shape of Heschl's gyrus. J. Neurosci. 31, 14067–14075.
Da Costa, S., van der Zwaag, W., Miller, L.M., Clarke, S., Saenz, M., 2013. Tuning in to sound: frequency-selective attentional filter in human primary auditory cortex. J. Neurosci. 33, 1858–1863.
De Martino, F., Moerel, M., Ugurbil, K., Goebel, R., Yacoub, E., Formisano, E., 2015. Frequency preference and attention effects across cortical depths in the human primary auditory cortex. Proc. Natl. Acad. Sci. USA 112, 16036–16041.
De Martino, F., Moerel, M., Xu, J., van de Moortele, P.-F., Ugurbil, K., Goebel, R., Yacoub, E., Formisano, E., 2014. . High-resolution mapping of myeloarchitecture in vivo: localization of auditory areas in the human brain. Cerebral Cortex.
De Martino, F., Zimmermann, J., Muckli, L., Ugurbil, K., Yacoub, E., Goebel, R., 2013. Cortical depth dependent functional responses in humans at 7T: improved specificity with 3D GRASE. PLoS ONE 8, e60514.
de Zwart, J.A., Silva, A.C., van Gelderen, P., Kellman, P., Fukunaga, M., Chu, R., Koretsky, A.P., Frank, J.A., Duyn, J.H., 2005. Temporal dynamics of the BOLD fMRI impulse response. Neuroimage 24, 667–677.
Dechent, P., Frahm, J., 2000. Direct mapping of ocular dominance columns in human primary visual cortex. Neuroreport 11, 3247–3249.
Deistung, A., Schafer, A., Schweser, F., Biedermann, U., Turner, R., Reichenbach, J.R., 2013. Toward in vivo histology: a comparison of quantitative susceptibility mapping (QSM) with magnitude-, phase-, and R2*-imaging at ultra-high magnetic field strength. Neuroimage 65, 299–314.
Dick, F., Tierney, A.T., Lutti, A., Josephs, O., Sereno, M.I., Weiskopf, N., 2012. In vivo functional and myeloarchitectonic mapping of human primary auditory areas. J. Neurosci.: Off. J. Soc. Neurosci. 32, 16095–16105.
Dumoulin, S.O., 2015. Functional MRI of the visual system. In: Uludag, K., Ugurbil, K., Berliner, L. (Eds.), fMRI: From Nuclear Spins to Brain Functions. Springer, New York, 420–471.
Dumoulin, S.O., Visserr, H.B., Zuiderbaan, F., Luijten, W., Wandell, P.L., Petridou N, B.A., 2013. In vivo evidence for functional and anatomical stripe-based subdivisions in human V2 and. Society for Neuroscience, San Diego, V3.
Dumoulin, S.O., Wandell, B.A., 2008. Population receptive field estimates in human visual cortex. Neuroimage 39, 647–660.
Duong, T.Q., Kim, D.S., Ugurbil, K., Kim, S.G., 2001. Localized cerebral blood flow response at submillimeter columnar resolution. Proc. Natl. Acad. Sci. USA 98, 10904–10909.
Duong, T.Q., Yacoub, E., Adriany, G., Hu, X., Ugurbil, K., Kim, S.G., 2003. Microvascular BOLD contribution at 4 and 7 T in the human brain: gradient-echo and spin-echo fMRI with suppression of blood effects. Magn. Reson. Med. 49, 1019–1027.
Duong, T.Q., Yacoub, E., Adriany, G., Hu, X., Ugurbil, K., Vaughan, J.T., Merkle, H., Kim, S.-G., 2002. High-resolution, spin-echo BOLD, and CBF fMRI at 4 and 7 T. Magn. Reson. Med.: Off. J. Soc. Magn. Reson. Med. / Soc. Magn. Reson. Med. 48, 589–593.
Duvernoy, H.M., Delon, S., Vannson, J.L., 1981. Cortical blood vessels of the human brain. Brain Res. Bull. 7, 519–579.
Edelstein, W.A., Glover, G.H., Hardy, C.J., Redington, R.W., 1986. The intrinsic signal-to-noise ratio in NMR imaging. Magn. Reson. Med. 3, 604–618.
Eickhoff, S., Walters, N.B., Schleicher, A., Kril, J., Egan, G.F., Zilles, K., Watson, J.D.G., Amunts, K., 2005. High-resolution MRI reflects myeloarchitecture and cytoarchitecture of human cerebral cortex. Hum. Brain Mapp. 24, 206–215.
Elliot Smith, G., 1907. A new topographical survey of the human cerebral cortex, being an account of the distribution of the anatomically distinct cortical areas and their relationship to the cerebral sulci. J. Anat. Physiol. 41, 237.
Feinberg, D.A., Yacoub, E., 2012. The rapid development of high speed, resolution and precision in fMRI. Neuroimage 62, 720–725.
Felleman, D.J., Van Essen, D.C., 1991. Distributed hierarchical processing in the primate cerebral cortex. Cereb. Cortex 1, 1–47.
Fischl, B., Dale, A.M., 2000. Measuring the thickness of the human cerebral cortex from magnetic resonance images. Proc. Natl. Acad. Sci. USA 97, 11050–11055.
Fischl, B., Rajendran, N., Busa, E., Augustinack, J., Hinds, O., Yeo, B.T.T., Mohlberg, H., Amunts, K., Zilles, K., 2008. Cortical folding patterns and predicting cytoarchitecture. Cereb. Cortex 18, 1973–1980.
Fischl, B., Sereno, M.I., Tootell, R.B., Dale, A.M., 1999. High-resolution intersubject averaging and a coordinate system for the cortical surface. Hum. Brain Mapp. 8, 272–284.
Flechsig, P., 1901. Developmental localisation of the cerebral cortex in the human subject. Lancet, 1027–1029.
Formisano, E., Kim, D.S., Di Salle, F., van de Moortele, P.F., Ugurbil, K., Goebel, R., 2003. Mirror-symmetric tonotopic maps in human primary auditory cortex. Neuron 40, 859–869.
Fracasso, A., Koenraads, Y., Porro, G.L., Dumoulin, S.O., 2016a. Bilateral population receptive fields in congenital hemihydranencephaly. Ophthalmic Physiol. Opt. 36, 324–334.
Fracasso, A., Petridou, N., Dumoulin, S.O., 2016b. Systematic variation of population receptive field properties across cortical depth in human visual cortex. Neuroimage 139, 427–438.
Fracasso, A., van Veluw, S.J., Visser, F., Luijten, P.R., Spliet, W., Zwanenburg, J.J., Dumoulin, S.O., Petridou, N., 2016c. Lines of Baillarger in vivo and ex vivo: myelin contrast across lamina at 7T MRI and histology. Neuroimage 133, 163–175.
Fukuda, M., Moon, C.H., Wang, P., Kim, S.G., 2006. Mapping iso-orientation columns by contrast agent-enhanced functional magnetic resonance imaging: reproducibility, specificity, and evaluation by optical imaging of intrinsic signal. J Neurosci. 26, 11821–11832.
Gagnon, L., Sakad, i, S., Lesage, F., Musacchia, J.J., Lefebvre, J., Fang, Q., Yucel, Ma, Evans, K.C., Mandeville, E.T., Cohen-Adad, J., Polimeni, J.R., Yaseen, Ma, Lo, E.H., Greve, D.N., Buxton, R.B., Dale, aM., Devor, a, Boas, Da, 2015. Quantifying the microvascular origin of BOLD-fMRI from first principles with two-photon microscopy and an oxygen-sensitive nanoprobeJ. Neurosci. 35, 3663–3675.
Gennari, F., 1782. De peculiari structura cerebri nonnulisque ejus morbis. Ex Regio Typographeo, Parma.
Geyer, S., 2013. High-field magnetic resonance mapping of the border between primary motor (Area 4) and somatosensory (area 3a) cortex in ex-vivo and in-vivo human brains. Microstructural Parcellation of the Human Cerebral Cortex: From Brodmann's Post-Mortem Map to in Vivo Mapping with High-Field Magnetic Resonance Imaging, pp. 239–254.
Geyer, S., Weiss, M., Reimann, K., Lohmann, G., Turner, R., 2011. Microstructural parcellation of the human cerebral cortex - from Brodmann's post-mortem map to in vivo mapping with high-field magnetic resonance imaging. Front Hum. Neurosci. 5, 19.
Gholipour, A., Kehtarnavaz, N., Briggs, R., Devous, M., Gopinath, K., 2007. Brain functional localization: a survey of image registration techniques. IEEE Trans. Med. Imaging 26, 427–451.
Gilbert, C.D., Wiesel, T.N., 1983. Clustered intrinsic connections in cat visual cortex. J. Neurosci. 3, 1116–1133.
Glasser, M.F., Van Essen, D.C., 2011. Mapping human cortical areas in vivo based on myelin content as revealed by T1- and T2-weighted MRI. J. Neurosci. 31, 11597–11616.
Goa, P.L.E., Koopmans, P.J., Poser, B.A., Barth, M., Norris, D.G., 2014. . BOLD fMRI signal characteristics of S1- and S2-SSFP at 7 T. Front. Neurosci. 8, 49.
Goense, J., Bohraus, Y., Logothetis, N.K., 2016. fMRI at high spatial resolution: implications for BOLD-models. Front. Comput. Neurosci. 10, 66.
Goense, J., Merkle, H., Logothetis, N.K., 2012. High-resolution fMRI reveals laminar differences in neurovascular coupling between positive and negative BOLD responses. Neuron 76, 629–639.
Goense, J.B.M., Logothetis, N.K., 2006. Laminar specificity in monkey V1 using high-resolution SE-fMRI. Magn. Reson. Imaging 24, 381–392.
Goense, J.B.M., Zappe, A.-C., Logothetis, N.K., 2007. High-resolution fMRI of macaque V1. Magn. Reson Imaging 25, 740–747.
Goldman, P.S., Nauta, W.J., 1977. Columnar distribution of cortico-cortical fibers in the frontal association, limbic, and motor cortex of the developing rhesus monkey. Brain Res. 122, 393–413.
Goncalves, N.R., Ban, H., Sanchez-Panchuelo, R.M., Francis, S.T., Schluppeck, D., Welchman, A.E., 2015. 7 T FMRI reveals systematic functional organization for binocular disparity in dorsal visual cortex. J. Neurosci. 35, 3056–3072.
Goodyear, B.G., Menon, R.S., 2001. Brief visual stimulation allows mapping of ocular dominance in visual cortex using fMRI. Hum. Brain Mapp. 14, 210–217.
Graham, J., Lin, C.S., Kaas, J.H., 1979. Subcortical projections of six visual cortical areas in the owl monkey, Aotus trivirgatus. J. Comp. Neurol. 187, 557–580.
Grill-Spector, K., Malach, R., 2004. The human visual cortex. Annu. Rev. Neurosci. 27, 649–677.
Grinvald, A., Lieke, E., Frostig, R.D., Gilbert, C.D., Wiesel, T.N., 1986. Functional architecture of cortex revealed by optical imaging of intrinsic signals. Nature 324, 361–364.

Grinvald, A., Shoham, D., Shmuel, A., Glaser, D., Vanzetta, I., Shtoyerman, E., Slovin, H., Wijnbergen, C., Hildesheim, R., Arieli, A., 1999. In-vivo optical imaging of cortical architecture and dynamicsModern Techniques in Neuroscience Research. Springer, 893–969.
Grinvald, A., Slovin, H., Vanzetta, I., 2000. Non-invasive visualization of cortical columns by fMRI. Nat. Neurosci. 3, 105–107.
Guidi, M., Huber, L., Lampe, L., Gauthier, C.J., Möller, H.E., 2016. Lamina-dependent calibrated BOLD response in human primary motor cortex. Neuroimage 141, 250–261.
Gutteling, T.P., Petridou, N., Dumoulin, S.O., Harvey, B.M., Aarnoutse, E.J., Kenemans, J.L., Neggers, S.F., 2015. Action preparation shapes processing in early visual cortex. J Neurosci. 35, 6472–6480.
Harel, N., Lin, J., Moeller, S., Ugurbil, K., Yacoub, E., 2006. Combined imaging-histological study of cortical laminar specificity of fMRI signals. Neuroimage 29, 879–887.
Harmer, J., Sanchez-Panchuelo, R.M., Bowtell, R., Francis, S.T., 2012. Spatial location and strength of BOLD activation in high-spatial-resolution fMRI of the motor cortex: a comparison of spin echo and gradient echo fMRI at 7T. NMR Biomed. 25, 717–725.
Harvey, B.M., Dumoulin, S.O., 2011. The Relationship between cortical magnification factor and population receptive field size in human visual cortex: constancies in cortical architecture. J. Neurosci. 31, 13604–13612.
Harvey, B.M., Dumoulin, S.O., 2016. Visual motion transforms visual space representations similarly throughout the human visual hierarchy. Neuroimage 127, 173–185.
Harvey, B.M., Fracasso, A., Petridou, N., Dumoulin, S.O., 2015. Topographic representations of object size and relationships with numerosity reveal generalized quantity processing in human parietal cortex. Proc. Natl. Acad. Sci. USA 112, 13525–13530.
Harvey, B.M., Klein, B.P., Petridou, N., Dumoulin, S.O., 2013. Topographic representation of numerosity in the human parietal cortex. Science 341, 1123–1126.
Heinzle, J., Koopmans, P.J., den Ouden, H.E.M.M., Raman, S.S., Stephan, K.E., During, P., Imaging, H.R., Heinzle, J., Me, C., 2016. A hemodynamic model for layered BOLD signals. Neuroimage 125, 556–570.
Hinds, O.P., Rajendran, N., Polimeni, J.R., Augustinack, J.C., Wiggins, G., Wald, L.L., Diana Rosas, H., Potthast, A., Schwartz, E.L., Fischl, B., 2008. Accurate prediction of V1 location from cortical folds in a surface coordinate system. Neuroimage 39, 1585–1599.
Hoffmann, M.B., Dumoulin, S.O., 2015. Congenital visual pathway abnormalities: a window onto cortical stability and plasticity. Trends Neurosci. 38, 55–65.
Hoffmann, M.B., Kaule, F.R., Levin, N., Masuda, Y., Kumar, A., Gottlob, I., Horiguchi, H., Dougherty, R.F., Stadler, J., Wolynski, B., Speck, O., Kanowski, M., Liao, Y.J., Wandell, B.A., Dumoulin, S.O., 2012. Plasticity and stability of the visual system in human achiasma. Neuron 75, 393–401.
Hoffmann, M.B., Stadler, J., Kanowski, M., Speck, O., 2009. Retinotopic mapping of the human visual cortex at a magnetic field strength of 7T. Clin. Neurophysiol. 120, 108–116.
Horton, J.C., Adams, D.L., 2005. The cortical column: a structure without a function. Philos. Trans. R Soc. Lond. B Biol. Sci. 360, 837–862.
Horton, J.C., Hocking, D.R., 1996. Anatomical demonstration of ocular dominance columns in striate cortex of the squirrel monkey. J. Neurosci. 16, 5510–5522.
Hua, J., Qin, Q., van Zijl, P.C.M., Pekar, J.J., Jones, C.K., 2014. Whole-brain three-dimensional T2-weighted BOLD functional magnetic resonance imaging at 7 T. Magn. Reson. Med. 72, 1530–1540.
Hubel, D.H., Wiesel, T.N., 1959. Receptive fields of single neurones in the cat's striate cortex. J. Physiol. 148, 574–591.
Hubel, D.H., Wiesel, T.N., 1962. Receptive fields, binocular interaction and functional architecture in the cat's visual cortex. J. Physiol. 160, 106–154.
Hubel, D.H., Wiesel, T.N., 1963. Shape and arrangement of columns in cat's striate cortex. J. Physiol. 165, 559–568.
Hubel, D.H., Wiesel, T.N., 1968. Receptive fields and functional architecture of monkey striate cortex. J. Physiol. 195, 215–243.
Hubel, D.H., Wiesel, T.N., 1969. Anatomical demonstration of columns in the monkey striate cortex. Nature 221, 747–750.
Hubel, D.H., Wiesel, T.N., 1972. Laminar and columnar distribution of geniculo-cortical fibers in the macaque monkey. J. Comp. Neurol. 146, 421–450.
Hubel, D.H., Wiesel, T.N., 1974. Uniformity of monkey striate cortex: a parallel relationship between field size, scatter, and magnification factor. J. Comp. Neurol. 158, 295–305.
Hubel, D.H., Wiesel, T.N., 1977. Ferrier lecture. functional architecture of macaque monkey visual cortex. Proc. R Soc. Lond. B Biol. Sci. 198, 1–59.
Huber, L., Goense, J., Kennerley, A.J., Ivanov, D., Krieger, S.N., Lepsien, J., Trampel, R., Turner, R., Möller, H.E., 2014. Investigation of the neurovascular coupling in positive and negative BOLD responses in human brain at 7 T. Neuroimage 97, 349–362.
Huber, L., Goense, J., Kennerley, A.J., Trampel, R., Guidi, M., Reimer, E., Ivanov, D., Neef, N., Gauthier, C.J., Turner, R., Möller, H.E., 2015. Cortical lamina-dependent blood volume changes in human brain at 7T. Neuroimage 107, 23–33.
Huth, A.G., de Heer, W.A., Griffiths, T.L., Theunissen, F.E., Gallant, J.L., 2016. Natural speech reveals the semantic maps that tile human cerebral cortex. Nature 532, 453–458.
Jin, T., Kim, S.-G., 2008. Cortical layer-dependent dynamic blood oxygenation, cerebral blood flow and cerebral blood volume responses during visual stimulation. Neuroimage 43, 1–9.
Jones, E.G., Burton, H., Porter, R., 1975. Commissural and cortico-cortical "columns" in the somatic sensory cortex of primates. Science 190, 572–574.
Jorge, J., Figueiredo, P., van der Zwaag, W., Marques, J.P., 2013. Signal fluctuations in fMRI data acquired with 2D-EPI and 3D-EPI at 7 T. Magn. Reson. Imaging 31, 212–220.
Kaes, T., 1907.Die Grosshirnrinde des Menschen in Ihren Massen und in Ihrem Fasergehalt.
Kemper, V.G., De Martino, F., Vu, A.T., Poser, B.A., Feinberg, D.A., Goebel, R., Yacoub, E., 2015. Sub-millimeter T2 weighted fMRI at 7 T: comparison of 3D-GRASE and 2D SE-EPI. Front. Neurosci. 9, 163.
Kennerley, A.J., Berwick, J., Martindale, J., Johnston, D., Papadakis, N., Mayhew, J.E., 2005. Concurrent fMRI and optical measures for the investigation of the hemodynamic response function. Magn. Reson. Med. 54, 354–365.
Kim, D.S., Duong, T.Q., Kim, S.G., 2000. High-resolution mapping of iso-orientation columns by fMRI. Nat. Neurosci. 3, 164–169.
Kim, J.H., Khan, R., Thompson, J.K., Ress, D., 2013. Model of the transient neurovascular response based on prompt arterial dilation. J. Cereb. Blood Flow. Metab. 33, 1429–1439.
Kim, S.-G., Ogawa, S., 2012. Biophysical and physiological origins of blood oxygenation level-dependent fMRI signals. J. Cereb. Blood Flow. Metab. 32, 1188–1206.
Klein, A., Andersson, J., Ardekani, B.A., Ashburner, J., Avants, B., Chiang, M.C., Christensen, G.E., Collins, D.L., Gee, J., Hellier, P., Song, J.H., Jenkinson, M., Lepage, C., Rueckert, D., Thompson, P., Vercauteren, T., Woods, R.P., Mann, J.J., Parsey, R.V., 2009. Evaluation of 14 nonlinear deformation algorithms applied to human brain MRI registration. Neuroimage 46, 786–802.
Klein, B.P., Harvey, B.M., Dumoulin, S.O., 2014. Attraction of position preference by spatial attention throughout human visual cortex. Neuron 84, 227–237.
Kok, P., Bains, L.J., van Mourik, T., Norris, D.G., de Lange, F.P., 2016. Selective activation of the deep layers of the human primary visual cortex by top-down feedback. Curr. Biol. 26, 371–376.
Kolasinski, J., Makin, T.R., Jbabdi, S., Clare, S., Stagg, C.J., Johansen-Berg, H., 2016. Investigating the stability of fine-grain digit somatotopy in individual human participants. J. Neurosci. 36, 1113–1127.
Koopmans, P.J., Barth, M., Norris, D.G., 2010. Layer-specific BOLD activation in human V1. Hum. Brain Mapp. 31, 1297–1304.
Koopmans, P.J., Barth, M., Orzada, S., Norris, D.G., 2011. Multi-echo fMRI of the cortical laminae in humans at 7 T. Neuroimage 56, 1276–1285.
Koopmans, P.J., Manniesing, R., Niessen, W.J., Viergever, M.A., Barth, M., 2008. MR venography of the human brain using susceptibility weighted imaging at very high field strength. MAGMA 21, 149–158.
Kruger, G., Glover, G.H., 2001. Physiological noise in oxygenation-sensitive magnetic resonance imaging. Magn. Reson. Med. 46, 631–637.
le Gros Clark, W.E., Sunderland, S., 1939. Structural changes in the isolated visual cortex. J. Anat. 73, (563-574.563).
Lee, A.T., Glover, G.H., Meyer, C.H., 1995. Discrimination of large venous vessels in time-course spiral blood-oxygen-level-dependent magnetic-resonance functional neuroimaging. Magn. Reson. Med. 33, 745–754.
Lu, H., Hua, J., van Zijl, P.C.M., 2013. Noninvasive functional imaging of cerebral blood volume with vascular-space-occupancy (VASO) MRI. NMR Biomed. 26, 932–948.
Lu, H., Van Zijl, P.C.M., 2005. Experimental measurement of extravascular parenchymal BOLD effects and tissue oxygen extraction fractions using multi-echo VASO fMRI at 1.5 and 3.0 T. Magn. Reson. Med 53, 808–816.
Lutti, A., Dick, F., Sereno, M.I., Weiskopf, N., 2014. Using high-resolution quantitative mapping of R1 as an index of cortical myelination. Neuroimage 93 (Pt 2), 176–188.
Malonek, D., Grinvald, A., 1996. Interactions between electrical activity and cortical microcirculation revealed by imaging spectroscopy: implications for functional brain mapping. Science 272, 551–554.
Markuerkiaga, I., Barth, M., Norris, D.G., 2016. A cortical vascular model for examining the specificity of the laminar BOLD signal. Neuroimage 132, 491–498.
Marques, J.P., Gruetter, R., 2013. New developments and applications of the MP2RAGE sequence–focusing the contrast and high spatial resolution R1 mapping. PLoS ONE 8, e69294.
Martuzzi, R., van der Zwaag, W., Dieguez, S., Serino, A., Gruetter, R., Blanke, O., 2015. Distinct contributions of Brodmann areas 1 and 2 to body ownership. Soc. Cogn. Affect Neurosci. 10, 1449–1459.
Martuzzi, R., van der Zwaag, W., Farthouat, J., Gruetter, R., Blanke, O., 2014. Human finger somatotopy in areas 3b, 1, and 2: a 7T fMRI study using a natural stimulus. Hum. Brain Mapp. 35, 213–226.
Menon, R.S., 2002. Postacquisition suppression of large-vessel BOLD signals in high-resolution fMRI. Magn. Reson. Med. 47, 1–9.
Menon, R.S., Goodyear, B.G., 1999. Submillimeter functional localization in human striate cortex using BOLD contrast at 4 T: implications for the vascular point-spread function. Magn. Reson. Med. 41, 230–235.
Menon, R.S., Ogawa, S., Strupp, J.P., Ugurbil, K., 1997. Ocular dominance in human V1 demonstrated by functional magnetic resonance imaging. J. Neurophysiol. 77, 2780–2787.
Moerel, M., De Martino, F., Ugurbil, K., Yacoub, E., Formisano, E., 2015. Processing of frequency and location in human subcortical auditory structures. Sci. Rep. 5, 17048.
Moon, C.H., Fukuda, M., Kim, S.G., 2013. Spatiotemporal characteristics and vascular sources of neural-specific and -nonspecific fMRI signals at submillimeter columnar resolution. Neuroimage 64, 91–103.
Moon, C.H., Fukuda, M., Park, S.H., Kim, S.G., 2007. Neural interpretation of blood oxygenation level-dependent fMRI maps at submillimeter columnar resolution. J Neurosci. 27, 6892–6902.
Mountcastle, V., Berman, A., Davies, P., 1955. Topographic organization and modality representation in first somatic area of cat's cerebral cortex by method of single unit analysis. Am. J. Physiol. 183, 464.
Mountcastle, V.B., 1957. Modality and topographic properties of single neurons of cat's

somatic sensory cortex. J. Neurophysiol. 20, 408–434.
Mountcastle, V.B., 1978. An organizing principle for cerebral function: the unit module and the distributed system. In: Edelman, S., Mountcastle, V.B. (Eds.), The Mindful Brain: Cortical Organization and the Group-Selective Theory of Higher Brain Function. MIT Press, Cambridge, Massachusetts and London, England, 7–50.
Muckli, L., De Martino, F., Vizioli, L., Petro, L.S., Smith, F.W., Ugurbil, K., Goebel, R., Yacoub, E., 2015. Contextual feedback to superficial layers of V1. Curr. Biol. 25, 2690–2695.
Nasr, S., Polimeni, J.R., Tootell, R.B., 2016. Interdigitated color- and disparity-selective columns within human visual cortical areas V2 and V3. J. Neurosci. 36, 1841–1857.
Ogawa, S., Menon, R.S., Tank, D.W., Kim, S.G., Merkle, H., Ellermann, J.M., Ugurbil, K., 1993. Functional brain mapping by blood oxygenation level-dependent contrast magnetic resonance imaging. A comparison of signal characteristics with a biophysical model. Biophys. J. 64, 803–812.
Olman, C.A., Harel, N., Feinberg, D.A., He, S., Zhang, P., Ugurbil, K., Yacoub, E., 2012. Layer-specific fMRI reflects different neuronal computations at different depths in human V1. PLoS ONE 7, e32536.
Olman, C.A., Van de Moortele, P.F., Schumacher, J.F., Guy, J.R., Ugurbil, K., Yacoub, E., 2010. Retinotopic mapping with spin echo BOLD at 7T. Magn. Reson. Imaging 28, 1258–1269.
Op de Beeck, H.P., Haushofer, J., Kanwisher, N.G., 2008. Interpreting fMRI data: maps, modules and dimensions. Nat. Rev. Neurosci. 9, 123–135.
Parkes, L.M., Schwarzbach, J.V., Bouts, A.A., Deckers, R.H., Pullens, P., Kerskens, C.M., Norris, D.G., 2005. Quantifying the spatial resolution of the gradient echo and spin echo BOLD response at 3 T. Magn. Reson. Med. 54, 1465–1472.
Peer, M., Salomon, R., Goldberg, I., Blanke, O., Arzy, S., 2015. Brain system for mental orientation in space, time, and person. Proc. Natl. Acad. Sci. USA 112, 11072–11077.
Petridou, N., Italiaander, M., van de Bank, B.L., Siero, J.C., Luijten, P.R., Klomp, D.W., 2012. Pushing the limits of high-resolution functional MRI using a simple high-density multi-element coil design. NMR Biomed. 26, 65–73.
Polimeni, J.R., Fischl, B., Greve, D.N., Wald, L.L., 2010. Laminar analysis of 7 T BOLD using an imposed spatial activation pattern in human V1. Neuroimage 52, 1334–1346.
Puckett, A.M., Aquino, K.M., Robinson, P.A., Breakspear, M., Schira, M.M., 2016. The spatiotemporal hemodynamic response function for depth-dependent functional imaging of human cortex. Neuroimage 139, 240–248.
Ress, D., Glover, G.H., Liu, J., Wandell, B., 2007. Laminar profiles of functional activity in the human brain. Neuroimage 34, 74–84.
Rockel, A.J., Hiorns, R.W., Powell, T.P., 1980. The basic uniformity in structure of the neocortex. Brain 103, 221–244.
Rockland, K.S., Lund, J.S., 1982. Widespread periodic intrinsic connections in the tree shrew visual cortex. Science 215, 1532–1534.
Rockland, K.S., Pandya, D.N., 1979a. Laminar origins and terminations of cortical connections of the occipital lobe in the rhesus monkey. Brain Res. 179, 3–20.
Rockland, K.S., Pandya, D.N., 1979b. Laminar origins and terminations of cortical connections of the occipital lobe in the rhesus monkey. Brain Res. 179, 3–20.
Salomon, R., Darulova, J., Narsude, M., van der Zwaag, W., 2014. Comparison of an 8-channel and a 32-channel coil for high-resolution fMRI at 7 T. Brain Topogr. 27, 209–212.
Sanchez Panchuelo, R.M., Schluppeck, D., Harmer, J., Bowtell, R., Francis, S., 2015. Assessing the spatial precision of SE and GE-BOLD contrast at 7 T. Brain Topogr. 28, 62–65.
Sanchez-Panchuelo, R.M., Francis, S., Bowtell, R., Schluppeck, D., 2010. Mapping human somatosensory cortex in individual subjects with 7T functional MRI. J Neurophysiol. 103, 2544–2556.
Sanchez-Panchuelo, R.M., Francis, S.T., Schluppeck, D., Bowtell, R.W., 2012. Correspondence of human visual areas identified using functional and anatomical MRI in vivo at 7 T. J. Magn. Reson. Imaging 35, 287–299.
Sereno, M.I., Lutti, A., Weiskopf, N., Dick, F., 2013. Mapping the human cortical surface by combining quantitative T(1) with retinotopy. Cereb. Cortex 23, 2261–2268.
Setsompop, K., Feinberg, D.A., Polimeni, J.R., 2016. Rapid brain MRI acquisition techniques at ultra-high fields. NMR Biomed.
Shipp, S., 2007. Structure and function of the cerebral cortex. Curr. Biol. 17, R443–R449.
Shmuel, A., Chaimow, D., Raddatz, G., Ugurbil, K., Yacoub, E., 2010. Mechanisms underlying decoding at 7 T: ocular dominance columns, broad structures, and macroscopic blood vessels in V1 convey information on the stimulated eye. Neuroimage 49, 1957–1964.
Shmuel, A., Yacoub, E., Chaimow, D., Logothetis, N.K., Ugurbil, K., 2007. Spatio-temporal point-spread function of fMRI signal in human gray matter at 7 T. Neuroimage 35, 539–552.
Siero, J.C., Petridou, N., Hoogduin, H., Luijten, P.R., Ramsey, N.F., 2011. Cortical depth-dependent temporal dynamics of the BOLD response in the human brain. J Cereb. Blood Flow. Metab. 31, 1999–2008.
Siero, J.C., Ramsey, N.F., Hoogduin, H., Klomp, D.W., Luijten, P.R., Petridou, N., 2013. BOLD specificity and dynamics evaluated in humans at 7 T: comparing gradient-echo and spin-echo hemodynamic responses. PLoS ONE 8, e54560.
Siero, J.C.W., Hendrikse, J., Hoogduin, H., Petridou, N., Luijten, P., Donahue, M.J., 2015. Cortical depth dependence of the BOLD initial dip and poststimulus undershoot in human visual cortex at 7 T. Magn. Reson. Med. 73, 2283–2295.
Siero, J.C.W., Hermes, D., Hoogduin, H., Luijten, P.R., Ramsey, N.F., Petridou, N., 2014. BOLD matches neuronal activity at the mm scale: a combined 7T fMRI and ECoG study in human sensorimotor cortex. Neuroimage 101, 177–184.
Silva, A.C., Lee, S.P., Iadecola, C., Kim, S.G., 2000. Early temporal characteristics of cerebral blood flow and deoxyhemoglobin changes during somatosensory stimulation. J. Cereb. 20, 201–206.
Sincich, L.C., Horton, J.C., 2005. The circuitry of V1 and V2: integration of color, form, and motion. Annu. Rev. Neurosci. 28, 303–326.
Sun, P., Ueno, K., Waggoner, R.A., Gardner, J.L., Tanaka, K., Cheng, K., 2007. A temporal frequency-dependent functional architecture in human V1 revealed by high-resolution fMRI. Nat. Neurosci. 10, 1404–1406.
Talairach, J., Tournoux, P., 1988. Co-Planar Stereotaxic Atlas of the Human Brain. Thieme, New York.
Tardif, C.L., Schäfer, A., Waehnert, M., Dinse, J., Turner, R., Bazin, P.-L., 2015. Multi-contrast multi-scale surface registration for improved alignment of cortical areas. Neuroimage 111, 107–122.
Thunell, E., van der Zwaag, W., Ogmen, H., Plomp, G., Herzog, M.H., 2016. Retinotopic encoding of the Ternus-Pikler display reflected in the early visual areas. J. Vis. 16, 26.
Tian, P., Teng, I.I.C., May, L.D.L., Kurz, R., Lu, K., Scadeng, M., Hillman, E.M.C., De Crespigny, A.J., D'Arceuil, H.E., Mandeville, J.B., Marota, J.Ja, Rosen, B.R., Liu, T.T., Boas, Da, Buxton, R.B., Dale, A.M., Devor, A., 2010. Cortical depth-specific microvascular dilation underlies laminar differences in blood oxygenation level-dependent functional MRI signal. Proc. Natl. Acad. Sci. 107, 15246–15251.
Tigges, J., Tigges, M., Perachio, A.A., 1977. Complementary laminar terminations of afferents to area 17 originating in area 18 and in the lateral geniculate nucleus in squirrel monkey. J. Comp. Neurol. 176, 87–100.
Tootell, R.B., Dale, A.M., Sereno, M.I., Malach, R., 1996. New images from human visual cortex. Trends Neurosci. 19, 481–489.
Trampel, R., Ott, D.V.M., Turner, R., 2011. Do the congenitally blind have a stria of Gennari? First intracortical insights in vivo. Cerebral Cortex 21, 2075–2081.
Triantafyllou, C., Hoge, R.D., Krueger, G., Wiggins, C.J., Potthast, A., Wiggins, G.C., Wald, L.L., 2005. Comparison of physiological noise at 1.5 T, 3 T and 7 T and optimization of fMRI acquisition parameters. Neuroimage 26, 243–250.
Triantafyllou, C., Hoge, R.D., Wald, L.L., 2006. Effect of spatial smoothing on physiological noise in high-resolution fMRI. Neuroimage 32, 551–557.
Ts'o, D.Y., Frostig, R.D., Lieke, E.E., Grinvald, A., 1990. Functional organization of primate visual cortex revealed by high resolution optical imaging. Science 249, 417–420.
Turner, R., 2002. How much cortex can a vein drain? Downstream dilution of activation-related cerebral blood oxygenation changes. Neuroimage 16, 1062–1067.
Uludağ, K., Müller-Bierl, B., Uğurbil, K., 2009. An integrative model for neuronal activity-induced signal changes for gradient and spin echo functional imaging. Neuroimage 48, 150–165.
van der Zwaag, W., Francis, S., Head, K., Peters, A., Gowland, P., Morris, P., Bowtell, R., 2009a. fMRI at 1.5 3 and 7 T: characterising BOLD signal changes. Neuroimage 47, 1425–1434.
van der Zwaag, W., Marques, J.P., Hergt, M., Gruetter, R., 2009b. Investigation of high-resolution functional magnetic resonance imaging by means of surface and array radiofrequency coils at 7 T. Magn. Reson Imaging 27, 1011–1018.
van der Zwaag, W., Gruetter, R., Martuzzi, R., 2015a. Stroking or Buzzing? A Comparison of Somatosensory Touch Stimuli Using 7 T fMRI. PLoS ONE 10, e0134610.
van der Zwaag, W., Jorge, J., Butticaz, D., Gruetter, R., 2015b. Physiological noise in human cerebellar fMRI. MAGMA 28, 485–492.
Vanduffel, W., Zhu, Q., Orban, G.A., 2014. Monkey cortex through fMRI glasses. Neuron 83, 533–550.
Vanzetta, I., Slovin, H., Omer, D.B., Grinvald, A., 2004. Columnar resolution of blood volume and oximetry functional maps in the behaving monkey; implications for FMRI. Neuron 42, 843–854.
Vogt, C., Vogt, O., 1919. Allgemeinere ergbnisse unserer Hirnforschung. J. Psychol. Neurol. 25, 399–462.
Vogt, O., 1910. Die myeloarchitektonische Felderung des menschlichen Stirnhirns. J. Psychol. Neurol. 15, 221–232.
von Economo, C.F., Koskinas, G.N., 1925. Die cytoarchitektonik der hirnrinde des erwachsenen menschen. J. Springer, Vienna.
Waehnert, M.D., Dinse, J., Schäfer, A., Geyer, S., Bazin, P.-L., Turner, R., Tardif, C.L., 2016. A subject-specific framework for in vivo myeloarchitectonic analysis using high resolution quantitative MRI. Neuroimage 125, 94–107.
Waehnert, M.D., Dinse, J., Weiss, M., Streicher, M.N., Waehnert, P., Geyer, S., Turner, R., Bazin, P.-L., 2014. Anatomically motivated modeling of cortical laminae. Neuroimage 93 (Pt 2), 210–220.
Walters, N.B., Egan, G.F., Kril, J.J., Kean, M., Waley, P., Jenkinson, M., Watson, J.D.G., 2003. In vivo identification of human cortical areas using high-resolution MRI: an approach to cerebral structure-function correlation. Proc. Natl. Acad. Sci. USA 100, 2981–2986.
Wandell, B.A., Dumoulin, S.O., Brewer, A.A., 2007. Visual field maps in human cortex. Neuron 56, 366–383.
Wang, Z., Roe, A.W., 2012. Columnar specificity of microvascular oxygenation and blood flow response in primary visual cortex: evaluation by local field potential and spiking activity. J. Cereb. Blood Flow. Metab. 32, 6–16.
Williams, R.W., Hogan, D., Garraghty, P.E., 1994. Target recognition and visual maps in the thalamus of achiasmatic dogs. Nature 367, 637–639.
Wong-Riley, M., 1979. Columnar cortico-cortical interconnections within the visual system of the squirrel and macaque monkeys. Brain Res. 162, 201–217.
Woolsey, T.A., Rovainen, C.M., Cox, S.B., Henegar, M.H., Liang, G.E., Liu, D., Moskalenko, Y.E., Sui, J., Wei, L., 1996. Neuronal units linked to microvascular modules in cerebral cortex: response elements for imaging the brain. Cereb. Cortex 6, 647–660.
Yacoub, E., Duong, T.Q., Moortele, P.-F.V.D., Lindquist, M., Adriany, G., Kim, S.-G., Uğurbil, K.m., Hu, X., Van De Moortele, P.-F., Lindquist, M., Adriany, G., Kim, S.-G., Uğurbil, K., Hu, X., 2003. Spin-echo fMRI in humans using high spatial resolutions and high magnetic fields. Magn. Reson. Med. 49, 655–666.
Yacoub, E., Harel, N., Ugurbil, K., 2008. High-field fMRI unveils orientation columns in

humans. Proc. Natl. Acad. Sci. USA 105, 10607–10612.
Yacoub, E., Shmuel, A., Logothetis, N., Ugurbil, K., 2007. Robust detection of ocular dominance columns in humans using Hahn Spin Echo BOLD functional MRI at 7 T. Neuroimage 37, 1161–1177.
Yacoub, E., Shmuel, A., Pfeuffer, J., Van De Moortele, P.F., Adriany, G., Andersen, P., Vaughan, J.T., Merkle, H., Ugurbil, K., Hu, X., 2001. Imaging brain function in humans at 7 T. Magn. Reson. Med. 45, 588–594.
Zhang, N., Zhu, X.H., Yacoub, E., Ugurbil, K., Chen, W., 2010. Functional MRI mapping neuronal inhibition and excitation at columnar level in human visual cortex. Exp. Brain Res. 204, 515–524.
Zhao, F., Wang, P., Hendrich, K., Kim, S.G., 2005. Spatial specificity of cerebral blood volume-weighted fMRI responses at columnar resolution. Neuroimage 27, 416–424.
Zilles, K., Amunts, K., 2010. Centenary of Brodmann's map - conception and fate. Nat. Rev. Neurosci. 11, 139–145.
Zilles, K., Palomero-Gallagher, N., Schleicher, A., 2004. Transmitter receptors and functional anatomy of the cerebral cortex. J. Anat. 205, 417–432.
Zimmermann, J., Goebel, R., De Martino, F., van de Moortele, P.-F., Feinberg, D., Adriany, G., Chaimow, D., Shmuel, A., Uğurbil, K., Yacoub, E., 2011. Mapping the organization of axis of motion selective features in human area MT using high-field fMRI. PLoS ONE 6, e28716.